Institut de recherche
Robert-Sauvé en santé
et en sécurité du travail

Characterization of Unintentionally Released Nanometric Particles in Various Workplaces

Maximilien Debia
Cyril Catto
Alan Fleck
Jean-Philippe Masse
Gilles L'Espérance
Brigitte Roberge

STUDIES AND RESEARCH PROJECTS

R-1133

CHEMICAL AND BIOLOGICAL HAZARD PREVENTION RESEARCH

OUR RESEARCH
is working for you !

The Institut de recherche Robert-Sauvé en santé et en sécurité du travail (IRSST), established in Québec since 1980, is a scientific research organization well-known for the quality of its work and the expertise of its personnel.

Mission

To contribute, through research, to the prevention of industrial accidents and occupational diseases and to the rehabilitation of affected workers;

To disseminate knowledge and serve as a scientific reference centre and expert;

To provide the laboratory services and expertise required to support the public occupational health and safety network.

Funded by the Commission des normes, de l'équité, de la santé et de la sécurité du travail, the IRSST has a board of directors made up of an equal number of employer and worker representatives.

To find out more

Visit our Web site for complete up-to-date information about the IRSST. All our publications can be downloaded at no charge.
www.irsst.qc.ca

To obtain the latest information on the research carried out or funded by the IRSST, subscribe to our publications:

- *Prévention au travail,* the free magazine published jointly by the IRSST and the CNESST (preventionautravail.com)
- InfoIRSST, the Institute's electronic newsletter

Legal Deposit
Bibliothèque et Archives nationales du Québec
2021

ISBN : 978-2-89797-147-2

IRSST – Communications and Knowledge Transfer Division
505 De Maisonneuve Blvd. West
Montréal, Québec
H3A 3C2
Phone: 514 288-1551
publications@irsst.qc.ca
www.irsst.qc.ca

Characterization of Unintentionally Released Nanometric Particles in Various Workplaces

Maximilien Debia[1], Cyril Catto[1], Alan Fleck[1], Jean-Philippe Masse[2], Gilles L'Espérance[2], Brigitte Roberge[3]

[1] Département de santé environnementale et santé au travail, École de santé publique, Université de Montréal

[2] Centre de caractérisation microscopique des matériaux, Polytechnique Montréal

[3] IRSST

STUDIES AND RESEARCH PROJECTS

R-1133

This study was funded by the IRSST. The conclusions and recommendations are solely those of the authors. This publication is a translation of the French original; only the original version (R-1075) is authoritative.

PEER REVIEW
In compliance with IRSST policy, the research results
published in this document have been peer-reviewed.

ACKNOWLEDGMENTS

The authors are grateful to the following individuals who contributed their expertise to this project or facilitated access to various workplaces: Jérôme Lavoué, Simon Aubin, Marie-France D'Amours, Isabelle Vézina, Ross Thuot, Jean-François Sauvé, Caroline Couture, Patrick E. Ryan, Kiet Anh Nguyen, Guillaume Lachapelle, François Couture, Renée Hallé, Marie-Josée Ferron, Julie McCabe, Geoffroy Denis, Siyu Tu and Paul Lambert.

Sincere thanks to all the staff of the companies and laboratories that allowed us to carry out this research.

This study is part of a joint initiative with a research team in France and aims to harmonize methods for assessing occupational exposure to nanometric particles. We would be remiss not to acknowledge the contributions of the researchers and collaborators involved in this ambitious project, which is called ExproPNano and is directed by Alain Garrigou. In particular, we thank Sabyne Audignon, Louis Galey and Alain Garrigou for their contribution to scientific exchanges on the subject.

ABSTRACT

Nanometric particles that are unintentionally released into the workplace are potentially toxic to workers. They can easily settle in the respiratory system and are distinctive because of their large surface area and high potential for causing pulmonary inflammation. The purpose of this study was to characterize unintentionally released nanometric particles (URNPs) found in six workplaces using a broad range of indicators.

Concentrations were assessed according to numerical and mass metrics using an array of direct-reading instruments (DRIs). Time-averaged measurements were also taken, based on the type of contaminant specific to each workplace. These measurements included (i) respirable and submicron carbon (elemental and organic) fractions, as well as respirable combustible dust from diesel engine exhaust (DEE) found in an underground mine (M1), in maintenance operations in an underground transit system (M2) and in a truck repair garage(M3); (ii) gravimetric measurements and concentrations of 12 metals (aluminum, cadmium, chromium, cobalt, copper, iron, magnesium, manganese, nickel, lead, vanadium, zinc) in fumes and metallic dust released in a foundry (M4), as well as in a machine shop (welding, grinding and cutting) (M5); (iii) paraffin wax (C_{18}-C_{36}) from fumes released in a wax-moulding shop (M6). In parallel, measurements for microscopy characterization were taken in the six workplaces.

For the measurements taken by DRIs, the daily number concentrations in the six workplaces ranged between 12,900 and 228,600 particles/cm³ and the mass concentrations between 0.01 and 3.22 mg/m³. In terms of number of particles, the underground mine was the environment with the highest concentrations, while the wax-moulding shop had the highest mass concentrations. In environments where DEE was found, daily concentrations of elemental carbon (EC) ranging from 0.002 to 0.503 mg/m³ were measured with DRIs.

For the time-averaged measurements, the concentrations of total carbon (TC) measured in this study were lower than the Quebec regulated level of 0.4 mg/m³ stipulated in the *Regulation Respecting Occupational Health and Safety in Mines*, with the exception of a level of 0.7 mg/m³ recorded in workplace M1. A comparison of the metal concentrations from workplaces M4 and M5 with the recommendations of the American Conference of Governmental Industrial Hygienists (ACGIH) found that all the concentrations were 10% below recommended levels, with the exception of one measurement of manganese (respirable fraction) in the foundry (M4). The paraffin wax fume concentrations measured were below the occupational exposure limit of 2 mg/m³ set by the ACGIH.

Workers exposed to DEE (M1, M2 and M3) are exposed to mostly nanometric-size airborne particles whose mass concentration is largely in the submicron fraction. In the presence of foundry fumes (M4), workers are exposed to airborne particles that are mostly nanometric in size and whose mass concentration is chiefly in the submicron fraction for chromium, cobalt, copper, iron, manganese, lead, vanadium and zinc. The workers in the machine shop (M5) are exposed to fumes and dust particles from machining, most of which are nanometric in size, but some of the processes they use generate larger, micrometric particles. The contribution of larger particles to the mass concentration is significant in this environment and, as a result, the mass concentration is to be found in the inhalable fraction, especially for chromium, copper, iron and nickel. Workers

in the wax shop (M6) are exposed to fumes that are chiefly nanometric in size and whose mass concentration is mostly in the submicron fraction.

Our innovative strategy enabled us to characterize the URNPs released in the different workplaces with respect to both number and mass concentrations. Microscopy studies on particle samples from the microscope grid taken with a Mini Particle Sampler® were used to characterize the particles collected based on their morphology and chemical composition.

TABLE OF CONTENTS

LIST OF TABLES

LIST OF FIGURES

LIST OF ACRONYMS AND ABBREVIATIONS

EC: Elemental Carbon

IARC: International Agency for Research on Cancer

OC: Organic Carbon

CM^2: Center for Characterization and Microscopy of Materials

TC: Total Carbon

CNC: Condensation nucleus counter

MMAD: Mass median aerodynamic diameter

MCE: Mixed cellulose esters

EDS: Energy dispersive X-ray spectroscopy

EEPS: Engine exhaust particle sizer

ELPI: Electrical low pressure impactor

DEE: Diesel engine exhaust

ESPUM: École de santé publique de l'Université de Montréal

GSD: Geometric standard deviation

FCAW: Flux-cored arc welding

FeNO: Exhaled nitric oxide fraction

FMPS: Fast mobility particle sizer

FEV_1: Maximum forced expiratory volume in 1 second

FVC: Forced vital capacity

GMAW: Gas metal arc welding

ICP-MS: Inductively coupled plasma mass spectrometry

DRI: Direct-reading instrument

INERIS: Institut national de l'environnement industriel et des risques (National Institute for Industrial Environment and Risks)(France)

IRSST: Institut de recherche Robert-Sauvé en santé et en sécurité du travail (Robert-Sauvé Research Institute for Occupational Health and Safety)(Québec)

LHIMP: Laboratoire d'hygiène industrielle et de métrologie des polluants (Laboratory for Industrial Hygiene and Pollutant Measurement)

SEM: Scanning electron microscopy

TEM: Transmission electron microscopy

GM: Geometric mean

MPS: Mini particle sampler

NRD: Nanoparticle respiratory deposition sampler

NIOSH: National Institute for Occupational Safety and Health

NP: Nanoparticle

URNP: Unintentionally released nanoparticle

MNP: Manufactured nanoparticle

UFP: Ultrafine particle

SMPS: Scanning mobility particle sizer

TIG: Tungsten inert gas

TWA: Time-weighted average exposure

OEL: Occupational exposure limit

1. INTRODUCTION

This research is a logical continuation of various studies conducted by the team at the Laboratoire d'hygiène industrielle et de métrologie des polluants (LHIMP) of the École de santé publique de l'Université de Montréal (ESPUM) on occupational exposure to nanoparticles.

The first, IRSST project 0099-7890, used condensation nucleus counters (CNCs) to characterize worker exposure to unintentionally released nanoparticles (URNPs) and manufactured nanoparticles (MNPs) (Debia, Beaudry, Weichenthal, Tardif and Dufresne, 2012a). The project demonstrated that CNCs are suitable for assessing nanoparticle concentrations, but that several uncertainties remain in assessing exposure to MNPs, mainly due to their agglomerated form.

Subsequently, IRSST project 2013-0059 focused on MNPs. It evaluated different methods for sampling and characterization of these particles in the air and on surfaces in workplaces (Debia, L'Espérance et al., 2017). In particular, it contributed to the study of specific tasks and industrial processes, as well as to the study of certain MNPs that have not yet been extensively examined, such as nanocellulose. These investigations have made it possible to propose a more precise strategy for evaluating MNP exposure using electron microscopy techniques requiring a minimum of pre-analysis manipulations.

The ExproPNano project, now under way, is funded by the French National Agency for Food, Environmental and Occupational Safety (ANSES) and is conducted in partnership with research teams in France under the direction of Alain Garrigou. This project aims to develop and test a harmonized approach to assessing occupational exposure to nanoparticles.

Based on this research, it appears that a characterization and control study of occupational nanoparticle exposure should include an assessment of mass and number concentrations, measurement of particle size distribution, and characterization by electron microscopy.

From this perspective, the present study provides new data on a wide range of indicators of exposure to URNPs.

2. STATE OF KNOWLEDGE

2.1 Definitions

Nanoparticles are usually defined as particles of matter between 1 and 100 nanometres (nm) in diameter (U.S. Environmental Protection Agency). There is a distinction between manufactured nanoparticles (MNPs) and unintentionally released ones (URNPs, also known as ultrafine particles or UFPs). The former are the result of commercial production in the field of nanotechnology, while the latter are natural (e.g. evaporation, erosion, volcanic eruption) or anthropogenic (welding fumes or diesel emissions) in origin. In industrial environments, URNPs are mainly generated during hot processes or combustion in the form of more or less agglomerated primary particles produced by condensation and nucleation.

URNPs are the specific subject of the investigations summarized in this report. It is understood, however, that the term "URNPs" here may sometimes include fractions of fine particles.

2.2 Health effects

Because of their small size, URNPs have the ability to penetrate blood vessels and then reach other targets such as the cardiovascular system, liver and central nervous system (Bakand, Hayes and Dechsakulthorn, 2012; Kreyling, Semmler-Behnke, Takenaka and Moller, 2013). They also have a larger surface area (compared with larger particles on a mass basis), a strong tendency to form deposits on the lungs, a high potential for lung inflammation and enhanced oxidant capacity (Frampton et al., 2004).

Some health effects from exposure to URNPs have been identified in epidemiological studies. These include: (i) mortality (Atkinson, Fuller, Anderson, Harrison and Armstrong, 2010; Breitner et al., 2011; Breitner et al., 2009); (ii) cardiovascular effects (e.g., arrhythmia, ischemia, blood pressure changes) (Barclay et al., 2009; Delfino et al., 2011; Delfino et al., 2009; Rich et al., 2012); (iii) respiratory effects (e.g., effects on lung function and allergies) (Andersen et al., 2008; de Hartog et al., 2010; Song et al., 2011).

The effects of URNP exposure on various measures of lung function (e.g., maximum 1-second forced expiratory volume [FEV1] and forced vital capacity [FVC]) and lung inflammation (e.g., exhaled nitric oxide fraction [FeNO]) have been examined in environmental exposure studies. Karottki et al. (2014) found that a 32,109-particle/cm^3 increase in exposure was associated with a 2.1% (95% IC: -3.7 to -0.2) reduction in the FEV1/FVC ratio in an elderly population in Denmark. Gong et al. compared levels of URNP exposure before and after the implementation of air quality control measures at the 2008 Beijing Olympics and studied the relationship between these levels and exhaled FeNO measurements in 125 young adults. The authors reported that a 5,340-particle/cm^3 increase was associated with a 23.3% increase in exhaled FeNO (95% CC: 12.9 to 39.0) immediately after exposure (Gong et al. 2014).

As for measurements conducted in a context of occupational exposure assessment, Haluza et al. found a significant decrease (-2.91 mL) in FEV1 in welders for each year of exposure (Haluza, Moshammer and Hochgatterer, 2014). Hoffmayer et al. reported changes in biomarkers in exhaled air following exposure to welding fumes. They suggested that lower respiratory tract irritant effects were increased in welders of mild steel parts using the flux-cored arc welding

process (FCAW) compared to those using gas metal arc welding (GMAW) (Hoffmeyer et al. 2012). Dierschke et al. also identified changes in the various inflammatory markers (LT-B4, IL-6 and IL-8) in the exhaled air or nasal lavage of workers exposed to welding fumes in a controlled-exposure chamber (Dierschke et al. 2017).

Moreover, several contaminants found mainly in nanoscale form are considered carcinogenic to humans. For example, diesel exhaust and welding fumes have been classified as Group 1 contaminants by the International Agency for Research on Cancer (IARC) (Benbrahim-Tallaa et al. 2012; Guha et al. 2017).

2.3 Occupational exposure assessment

Worker exposure to nanoparticles is assessed by different methods. The first is real-time measurement with a direct-reading instrument (DRI) that reports mass, number or surface area concentrations of fine and ultrafine particles. The second is the conventional method for assessing worker exposure; it is based on a set of measurements performed on samples taken in the worker's breathing zone, followed by analysis of the contaminants according to a mass metric. This second type, referred to here as "time-averaged measurement", is widely used to compare results with regulatory exposure or industrial hygiene standards.

2.3.1 Real-time measurement

2.3.1.1 Instrumentation

A condensation nucleus counter (CNC), such as a P-Trak® or CPC 3700 (TSI Inc.), can be used to measure number particle concentrations (particle count/cm³). Several papers have reported on the use of CNCs in the workplace and the external environment (Brouwer, Gijsbers and Lurvink, 2004; Cattaneo, Garramone, Taronna, Peruzzo and Cavallo, 2009; Cena and Peters, 2011; Debia, Neesham-Grenon, Mudaheranwa and Ragettli, 2016; Debia, Trachy-Bourget, et al., 2017; Dewalle, Vendel, Weulersse, Hervé and Decobert, 2010; Handy, Jackson, Robinson and Lafreniere, 2006; Schmoll, Peters and O'Shaughnessy, 2010; Szymczak, Menzel and Keck, 2007).

Light-scattering laser photometers such as the DustTrak™ (TSI Inc.) are used to estimate mass concentrations of different predefined aerosol particle size fractions (i.e., for different particle size classes). They are widely used for measuring dust in the outdoor environment or in various indoor environments, such as offices and industrial plants (Bello et al. 2009; Bello et al. 2010; Debia et al. 2016; Debia, Trachy-Bourget et al. 2017; Debia, Weichenthal and Dufresne 2014; Evans, Ku, Birch and Dunn 2010; Raynor et al. 2012).

Going up a notch in terms of size and cost, the scanning mobility particle sizer (SMPS), the fast mobility particle sizer (FMPS) and the electrical low pressure impactor (ELPI) have also been used in characterization studies (Bello et al. 2009; Bello et al. 2010; Brouwer et al. 2012; Dahm, Yencken and Schubauer-Berigan 2011; Debia, Beaudry, Weichenthal, Tardif and Dufresne 2012b; Koivisto 2010; Kuhlbusch, Neumann and Fissan 2004). These instruments measure both number and mass concentrations in different particle size classes. Aerosol particle size distribution is also a key parameter for characterizing the health risk of nanoparticles, considering

that, during inhalation, the site of deposition in the respiratory tract is strongly related to size (Ostiguy, Debia, Roberge and Dufresne, 2014).

2.3.1.2 Exposure levels

Viitanen et al. conducted a literature review on worker exposure to URNPs (Viitanen, Uuksulainen, Koivisto, Hameri and Kauppinen, 2017). They reported 72 studies that specifically measured occupational exposure and provided particle counts per cm³ using a DRI. The papers covered 314 occupational exposure situations including asphalt/bitumen work, machining, metal manufacturing, painting and coating, power plants, transportation and diesel exhaust, welding, office work, catering and cooking fumes, and various services. The authors reported that the highest concentrations were found during welding and other activities related to the metal industry, with concentrations that were over 100 times the average background levels, or more than 1,000,000 particles/cm³.

Debia et al. described the concentrations of URNPs released during various welding activities. They reported daily mean concentrations ranging from 50,000 to 150,000 particles/cm^3, with peaks reaching the instrument ceiling of 500,000 particles/cm^3 (Debia et al., 2014). Concentrations of more than 100,000 particles/cm³ were also measured in a carbon black production and pelletizing plant (Kuhlbusch and Fissan, 2006). Jarvela et al. looked at URNP emissions during the production of stainless steel and ferrochromium. They measured concentrations ranging from 58,000 to 662,000 particles/cm^3 (Järvelä et al., 2016). Freund et al. estimated peak concentrations of 467,000 particles/cm³ during paving activities (Freund, Zuckerman, Baum and Milek, 2012).

Jorgensen et al. used an FMPS to evaluate the number concentration and particle size distribution of particles during work in a tunnel. They reported geometric means (GMs) of 240,000 to 3,000,000 particles/cm^3 during welding operations. Mobility diameters at the maximum particle concentration were 10.8 nm during welding and 60.4 nm during finishing work (Jorgensen, Buhagen and Foreland, 2016).

Number concentrations of URNPs emitted by diesel engines have also been measured in several occupational exposure settings including port facilities (daily concentrations of 36,000 particles/cm^3 average and 67,000 particles/cm^3 maximum), school bus parking lots (116,000 particles/cm^3 average and 186,000 particles/cm^3 peak), and diesel locomotives (126,000 particles/cm^3 average and 693,000 particles/cm^3 peak) (Bujak-Pietrek, Mikolajczyk, Kaminska, Cieslak and Szadkowska-Stanczyk, 2016; Debia et al. 2016; Jeong, Traub and Evans, 2017).

Mass concentrations in different aerosol fractions were also measured using DRIs. Concentrations ranging from 22 to 483 µg/m³ of fine particles smaller than 1 µm (referred to as PM_1) were reported in a carbon black production and pelletizing plant (Kuhlbusch and Fissan, 2006). Geometric mean concentrations of 300 µg/m³ of $PM_{2.5}$ were measured at a welding school and a power plant (Kim, Magari, Herrick, Smith and Christiani, 2004). Particulate mass concentrations of diesel emissions have also been reported in the various settings mentioned above. In port facilities, mean daily concentrations of 40.4 µg/m³ and 37.7 µg/m³ were measured for the respirable and PM_1 fractions, respectively (Debia et al., 2016). In a school bus parking lot, mean daily concentrations ranging from 25 to 45 µg/m³ were also reported (Debia, Trachy-Bourget et al., 2017).

2.3.2 Time-averaged measurement

2.3.2.1 Instrumentation

Worker exposure to URNPs is also measured from various types of samples subjected to laboratory analysis. These measurements are used primarily to assess compliance with regulatory standards or to make comparisons with industrial hygiene recommendations. Possible analyses include gravimetric measurements for dust and fumes, inductively coupled plasma mass spectrometry (ICP-MS) for metal fumes, and specific thermo-optical analysis of elemental carbon (EC) and total carbon (TC) for DEE (TC = EC + organic carbon (OC)).

Time-averaged measurement may require particle size selectors, such as cyclones to sample the respirable fractions and impactors to select the submicronic particles (PM_1). For example, methods for assessing exposure to DEE include measurement of the respirable or PM_1 fractions of EC and TC (NIOSH, 2003).

There is also the nanoparticle respiratory deposition sampler (NRD), designed to specifically sample the nanoparticle fraction deposited in the respiratory tract. Cena et al. tested this instrument to assess the Cr, Ni and Mn exposures of welders in comparison to conventional measurements using a 37-mm cassette (Cena, Chisholm, Keane and Chen, 2015). They concluded that most of the Cr and more than half of the Ni and Mn consisted of fume particles less than 300 nm in aerodynamic diameter. The authors proposed that future work could focus on sampling these fine and ultrafine fractions (which tend to deposit in the respiratory tract) in order to establish links with measured health effects.

2.3.2.2 Exposure levels

Readers interested in obtaining more quantitative information on worker exposure to the various contaminants characterized by a dominant ultrafine fraction may refer to review documents or scientific articles. One example is the IARC document on exposure to diesel engine exhaust (International Agency for Research on Cancer, 2014), which reports on EC exposure levels measured in many workplaces. These environments include the mining industry, where concentrations ranging from 148 to 637 µg/m³ were reported for underground work and from 3.5 to 23 µg/m³ for surface work. Other literature documents levels of exposure to welding fumes. Hoffmeyer et al. (2012), for example, indicated that welders using FCAW are exposed to significantly higher respirable fume concentrations than those using GMAW, with median concentrations of 7.14 mg/m³ and 3.05 mg/m³, respectively.

2.3.3 Microscopy analysis

Nanoparticle characterization by transmission electron microscopy (TEM) or scanning electron microscopy (SEM), followed by energy dispersive X-ray spectroscopy (EDS), is also performed on samples mounted on grids, filters or other media (Debia, L'Espérance, et al., 2017; Kouassi et al., 2017). Members of our research team have performed numerous electron microscopy characterization studies. IRSST report R-1009 presents a review of methods for particle sampling and analysis by electron microscopy (Debia, L'Espérance, et al., 2017).

2.3.4 Metrology paradigm and evaluation strategy

Determining the most appropriate indicator of nanoparticle exposure remains a challenge today, due to their specificities and continuing uncertainty about which parameters are the most indicative of toxic effects. As mentioned earlier, two metrics dominate the measurements used to assess occupational exposure to nanoparticles: number measurement (particle count per cm^3) and mass measurement (mg/m^3).

Debia et al. (2016) demonstrated in a field study that the numerical metric accurately described seasonal and spatial differences in terms of DEF contamination. In a second study, number concentrations were also shown to correlate better with different determinants of exposure than mass concentrations of the same contaminant (Debia, Trachy-Bourget, et al., 2017). However, mass concentrations are widely used, and most regulations and recommendations issued are expressed in this metric. DRIs, which estimate mass concentrations, are therefore widely used in industrial hygiene. Kim et al. evaluated the predictive quality of a laser photometer (DustTrak™, TSI Inc.) by performing parallel gravimetric measurements. They concluded that these instruments are good predictors of gravimetric measurements, but that correction factors may be required, depending on the type of contaminant being assessed (Kim et al. 2004).

Viitanen et al. (2017) identified gaps in the assessment of exposure to URNPs and maintained that, due to the limited representativeness of the measurements and the differences in the way DRIs function, the current data do not allow the creation of job/exposure matrices specific to URNP exposure.

Consequently, there are still many uncertainties surrounding the interpretation of exposure data; further studies are needed. In this context and as a logical continuation of the work already done, the present research aims to fill certain gaps (little usable data on URNP exposure, workplaces still insufficiently studied), while taking into account the latest developments in exposure studies and nanoparticle measurement in particular (comparison of various indicators, need for standardization of strategies). It provides new data that will make it easier to identify, through the critical application of an original and innovative approach, the health risks attributable to URNPs.

3. RESEARCH OBJECTIVES

The objective was to evaluate various situations of potential exposure to URNPs in six Québec workplaces. This was carried out using an innovative strategy combining various exposure indicators to characterize and study, both qualitatively and quantitatively, the aerosols to which workers are potentially exposed.

More specifically, our aim was to:

- measure many different indicators and produce as accurate a picture of URNP concentrations as possible;
- characterize the morphology and chemical composition of URNPs by electron microscopy;
- assess the evaluation strategy used.

4. METHODOLOGY

The same measurement plan, consisting of a combination of real-time and time-averaged measurements, was repeated six times in six different workplaces with two simultaneous sampling sites.

4.1 Workplaces

The six workplaces assessed were ones with a high probability of finding URNPs. These workplaces were selected based on data already produced by the research team and on data from the literature. Three are affected by the presence of diesel-powered equipment: an underground gold mine (M1), an underground environment with diesel locomotives and diesel auxiliary engines (M2), and a truck repair and maintenance shop (M3). The other three are different areas within the same company: a stainless steel foundry (M4), a machine shop using TIG welding, grinding and cutting (M5), and a paraffin wax casting shop (M6). M4 and M5 had metal fumes and dust while M6 had paraffin wax fumes. Table 1 summarizes the six workplaces.

Table 1. Workplaces and main URNPs assessed

Workplace	Description	URNPs
M1	Underground gold mine	Diesel engine exhaust
M2	Underground environment with diesel engines	Diesel engine exhaust
M3	Truck repair shop	Diesel engine exhaust
M4	Steel foundry	Metal fumes and dust
M5	Machine shop (TIG welding, grinding, cutting)	Metal fumes and dust
M6	Wax-moulding shop	Paraffin wax fumes

4.2 Measuring devices

The measuring devices were installed in two portable suitcases specially designed for this research project. Figure 1 shows an example of a setup. Each suitcase was fitted identically, but some adjustments were made depending on the type of contaminants and workplace. Contents:

i. a set of DRIs for recording a wide range of parameters in real time throughout the process;

ii. sampling trains for subsequent analysis of different sample media to produce time-averaged measurements of the aerosol mass concentrations in different fractions.

At the same time, samples were taken and placed on microscopic grids for subsequent analysis of particle morphology and elemental chemical characterization.

Figure 1. Environmental measuring setup.

4.2.1 Real-time measurements

Table 2 lists the DRIs used in this project, along with the characteristics of each and the parameters measured. With the exception of the engine exhaust particle sizer (EEPS), shown in Figure 2, the instruments were arranged in the cases described above and the sampling heads were held vertical outside the case with aluminum rods (Figure 1).

CNCs (P-Trak® 8525, TSI Inc.) and laser photometers (DustTrak™ DRX and DustTrak™ 8520, TSI Inc.) were used for each procedure. These instruments measure the number (particles/cm^3) and mass (mg/m^3) concentrations of fine and ultrafine particles for different fractions (PM_1, $PM_{2.5}$, PM_{Resp}, PM_{10} and PM_{tot}). The Airtec uses light transmission to obtain equivalent EC measurements. This type of instrument has been used in environments where DEE was being measured (M1, M2 and M3). The Airtecs were connected with impactors and with series-connected cyclones to specifically measure submicron fractions of elemental carbon (EC_1). In these workplaces, the DustTrak™ 8520 units were connected to nylon cyclones to specifically measure respirable fractions (PM_{Resp}), with the instrument pump adjusted to 1.7 L/min. At M4, M5 and M6, the DustTrak™ 8520 units were equipped with a 10-µm impactor. The EEPS was used from time to time at M3, M4, M5 and M6; it could not be transported to M1 or M2.

The instrumentation was regularly maintained and calibrated, in accordance with good industrial hygiene practices, for the purposes of this investigation. The instruments were set to record measurements every 10 seconds during operation.

Table 2. Direct-reading instruments (DRIs)

Model	Parameter measured (unit of concentration)	Type of instrument	Measured particle size (in nm)
P-Trak® 8525 (TSI Inc.)	Number concentration (particles/cm^3)	Condensation nucleus counter (CNC)	20 – 1000
DustTrak™ DRX 8533 (TSI Inc.)	Mass concentration (mg/m^3) for 4 particle size fractions (PM_1, $PM_{2.5}$, PM_{resp}, and PM_{10})	Laser photometer	100 – 15,000
DustTrak™ 8520	Mass concentration (mg/m^3)	Laser photometer	100 – 15,000
Airtec (FLIR)	EC mass concentration (mg/m^3)	Light transmission	< 1,000
EEPS 3090 (TSI Inc.)	Number concentrations (particles/cm$_3$) for 32 particle size fractions	Engine exhaust particle sizer	56 – 560

Figure 2. Engine exhaust particle sizer (EEPS).

4.2.2 Time-averaged measurement

Gravimetric and specific measurements were taken in the six workplaces. The sampling pumps were placed inside the suitcase, and the sampling heads were held upright outside the suitcase with aluminum rods (Figure 1).

Table 3 shows the parameters measured using the multi-device sampling approach in the six workplaces. The pumps used to draw air through the sampling medium were systematically calibrated before and after each sampling. These samples were all taken simultaneously and at the same time as the DRI measurements.

The mounting media were then analyzed at the laboratory of the Institut de recherche Robert-Sauvé en santé et en sécurité du travail (IRSST). TC and EC levels were measured using the method IRSST 388, which is equivalent to NIOSH Method 5040 (Version 3, 2003). Respirable

dust (D_R) and respirable combustible dust (CD_R) were analyzed gravimetrically, using the method IRSST 384. The concentrations of metals (aluminum, cadmium, chromium, cobalt, copper, iron, magnesium, manganese, nickel, lead, vanadium and zinc) were determined by inductively coupled plasma mass spectrometry (ICP-MS) using the method IRSST 362. Paraffin wax fumes (C_{18}-C_{36}) were also measured by the IRSST laboratory, but the analyses were done by the SGS Galson laboratory (East Syracuse, NY), using a method adapted from OSHA PV2047.

Table 3. Mounted-sample analyses performed for each visit to the workplaces

	Parameter measured	Sampling device
M1, M2 and M3	Respirable fractions of elemental carbon (EC_R), organic carbon (OC_R) and total carbon (TC_R)	Gilair pump (1.7 L/min) with a 37-mm closed cartridge and quartz fibre filter, equipped with a Dorr-Oliver cyclone
	PM_1 fractions of elemental carbon (EC_1), organic carbon (OC_1) and total carbon (TC_1)	Same setup with the addition of an impactor
	Respirable fractions of dust (D_R) and combustible dust (CD_R)	Gilair pump (1.7 L/min) with a 37-mm closed cartridge and quartz fibre filter, equipped with a Dorr-Oliver cyclone
M4, M5	Total and inhalable dust, and metals concentration (gravimetry and ICP-MS) Particle masses and metals impacted on filters: 50% cut-off diameter: 2.5 µm, 1.0 µm, 0.5 µm and 0.25 µm	Gilair pump (1.5 L/min), 37-mm closed cassette with mixed cellulose ester (MCE) filter and IOM cassette (SKC Inc.) with MCE filter Sioutas impactor and Leland Legacy pump (9 L/min), 25-mm and 37-mm MCE filters
M6	Total dust and C_{18}-C_{36} concentration Particle masses impacted on filters: 50% cut-off diameter: 2.5 µm, 1.0 µm, 0.5 µm and 0.25 µm	Gilair pump (1.5 L/min), 37-mm closed cartridge with fibreglass filters Sioutas impactor and Leland Legacy pump (9L/min), 25-mm and 37-mm fibreglass filters

4.2.3 Microscopy analysis

Aerosol samples on microscopy grids were taken using the Mini Particle Sampler® (MPS). This device, developed by the Institut national de l'environnement industriel et des risques (INERIS) in France, can sample on porous microscopy grids (R'mili et al., 2013b). It was used to collect the particles directly on numbered microscopy observation grids. A Gilair pump was used for sampling at a flow rate of 0.3 L/min. Three 1-minute samples were taken each day at M1, M4, M5 and M6. Two samples a day were taken at M2 and M3. TEM observations were then made against a bright field, and characterizations were performed through EDS analysis.

First, the grid was inspected for homogeneity of the deposit and distribution of particles and agglomerates. Subsequently, three holes were chosen for observation at a higher magnification. A 50X magnified image showing the locations of the selected holes and their surroundings was systematically recorded (Figure 3). Higher-magnification images were then captured for each selected hole to see the particle distribution there.

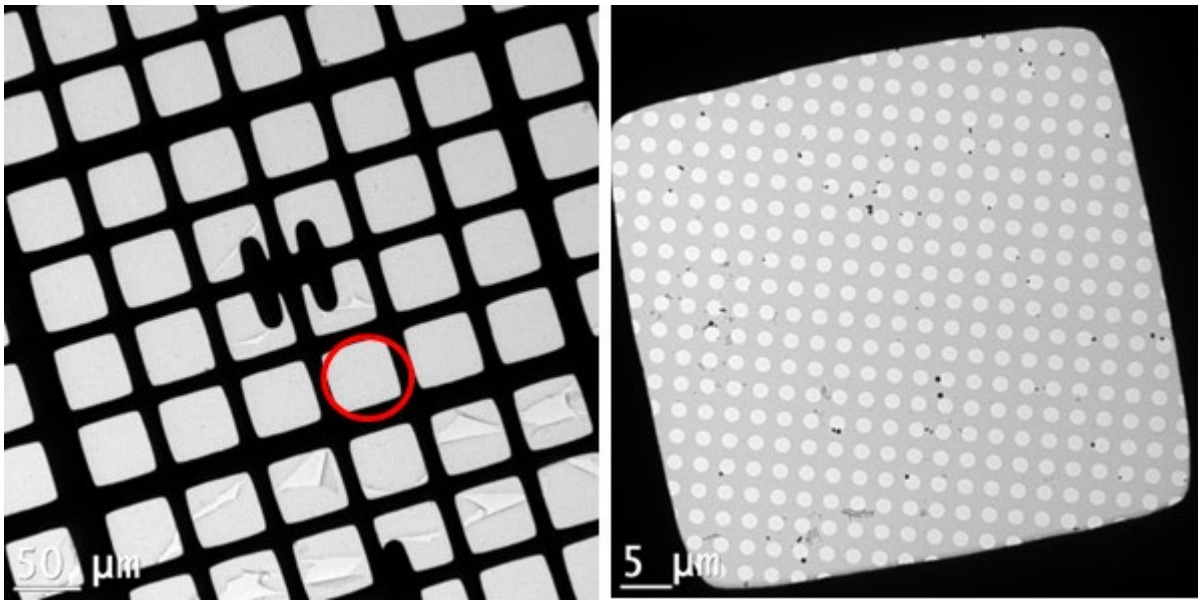

Figure 3. TEM bright-field images: low-magnification (50X) of a numbered grid (A) and high-magnification(400X) of a hole in the grid.

Particle analysis was then performed at a magnification of 5,000X to 25,000X. For each particle or particle agglomerate, an image was taken and an EDS analysis performed (Figure 4). Seven particles per hole were analyzed for three holes, for a total of 21 particles per grid. The particles were selected by the operator, randomly but with the aim of ensuring good representation of the diversity of particles found on the grid during the initial scan. For each image, the state of the particle (alone or agglomerated), its size and the elements present were recorded.

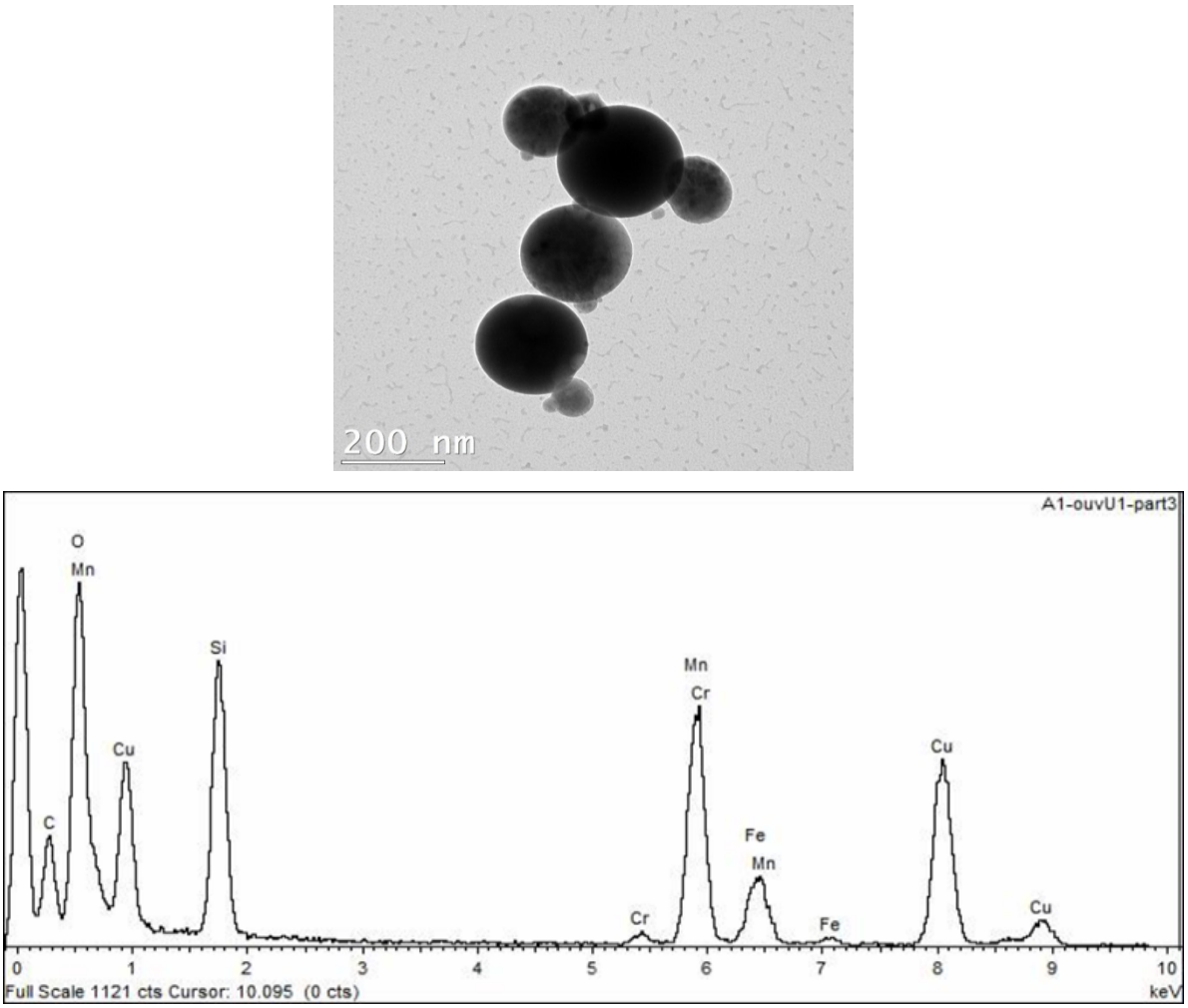

Figure 4. TEM high-magnification bright-field image of a particle agglomerate and corresponding EDS spectrum.

4.3 Data analysis

The geometric mean (GM), geometric standard deviation (GSD), and maxima (MAX) and minima (MIN) of the daily concentrations were used to describe the distributions of concentrations in the six workplaces. The undetected values were processed by dividing the quantification limit by the square root of 2. The distributions were represented in the form of boxplots. In each box, the central value represents the median while the lower and upper edges are the 1st and 3rd quartiles respectively and the ends of the moustaches are the maximum and minimum values or 1.5 times the interquartile range (between the 1st and 3rd quartiles). Values outside the zone of 1.5 times the interquartile range are represented by dots.

Mass median aerodynamic diameter (MMAD) calculations were performed for measurements taken with Sioutas impactors, with the assumption that the mass distribution follows a lognormal distribution as described by Hinds (1998).

To evaluate the monotonic relationship between the parameters, Spearman's correlation coefficients were calculated. Linear regression analyses were used to assess the relationships between certain parameters. Seasonal comparisons of concentrations were made using Student's *t*-test with log-transformed concentrations.

The significance level for statistical analyses was set at 5%. Most of the statistical and graphical analyses were performed using R software (version 3.4.2, R Development Core Team, Vienna, Austria).

5. RESULTS

5.1 Real-time measurement

5.1.1 Number concentrations

5.1.1.1 Condensation nucleus counters (P-Trak®)

The geometric means, geometric standard deviations, and minimum and maximum daily number concentrations measured with the P-Trak® in each of the six workplaces are presented in Table 4. Figure 5 shows the distribution of daily number concentrations measured with the P-Trak® in the workplaces. These concentrations varied considerably, with daily averages ranging from 12,900 to 228,600 particles/cm³. The three workplaces with the highest concentrations were, in descending order, the underground mine (M1), the foundry (M4) and the wax casting shop (M6), with averages of 128,200, 80,400 and 75,500 particles/cm³, respectively. The workplace with the lowest concentrations was the truck repair shop (M3) with a daily average of 22,800 particles/cm³. M4 had the highest GSD (2.3) while in M6 a GSD of 1.2 was calculated for the number concentrations.

Table 4. Descriptive statistics of daily number concentrations measured with P-Trak®

Workplace	n	GM (particles/cm^3)	GSD	Min (particles/cm^3)	Max (particles/cm^3)
M1	11	128,200	1.6	51,200	228,600
M2	10	32,800	1.8	12,900	58,600
M3	12	22,800	1.3	14,700	33,800
M4	12	80,400	2.3	23,700	262,200
M5	12	41,000	1.5	17,000	63,600
M6	12	75,500	1.2	50,600	105,700

n: number of daily averages
GM: geometric mean
GSD: geometric standard deviation
MIN: minimum MAX: maximum

Figure 6 shows the distributions of the instantaneous (averaged over one minute) number concentrations measured with the P-Trak® in each workplace. In M1, M2, M3, M4 and M5, concentrations of nearly 500,000 particles/cm³ were estimated, which is at the top of the instrument scale. At M6, relatively high levels (on the order of 75,000 particles/cm^3) were measured, but some homogeneity of concentrations was noted and none exceeded 350,000 particles/cm^3.

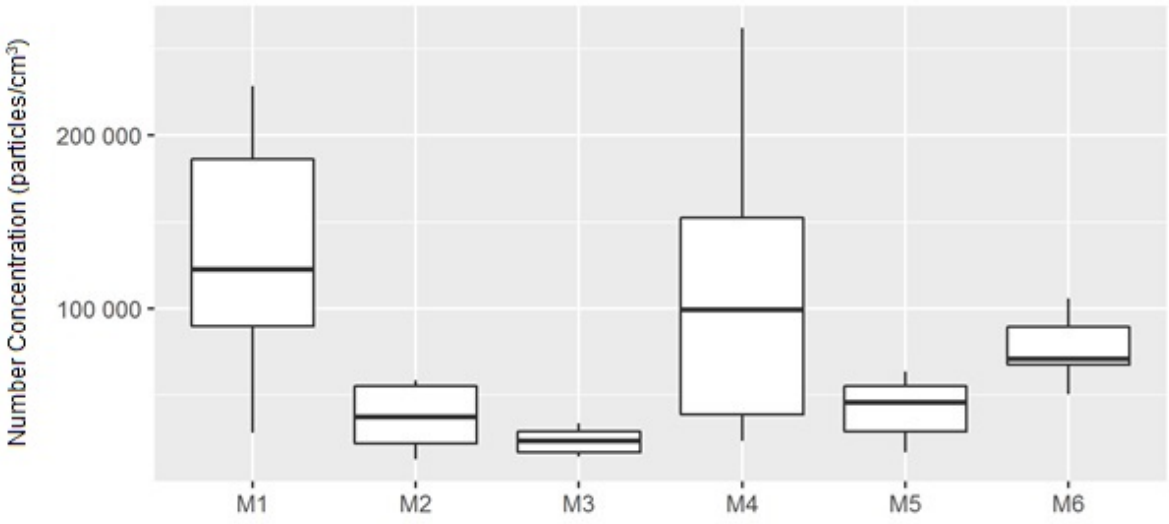

Figure 5. Distribution of daily number concentrations (particles/cm³) measured with P-Trak®.

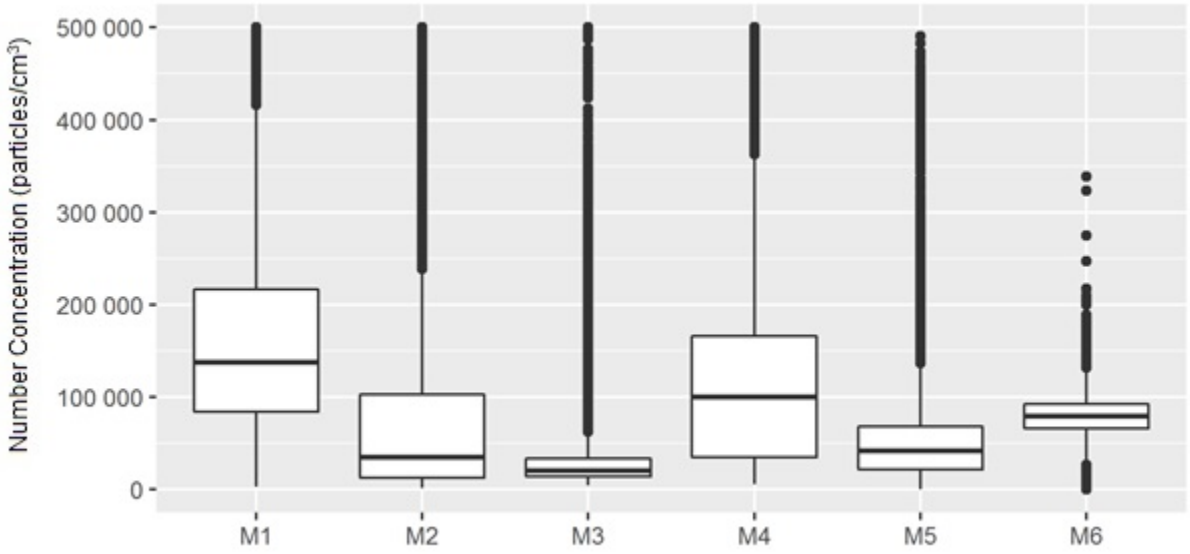

Figure 6. Distribution of instantaneous (one-minute averaged) number concentrations (particles/cm³) measured with P-Trak®.

Figure 7 gives an example, for each workplace, of the typical concentration profile using P-Trak® measurements. In general, many peak particle concentrations and relatively high levels can be seen throughout the sampling period for M1 and M6. In many workplaces, a decrease in particle emissions is easily observed during shutdowns (shown by blue arrows). For example, at M5,

when machining activities are stopped, the ventilation system brings about a rapid decrease in number concentrations.

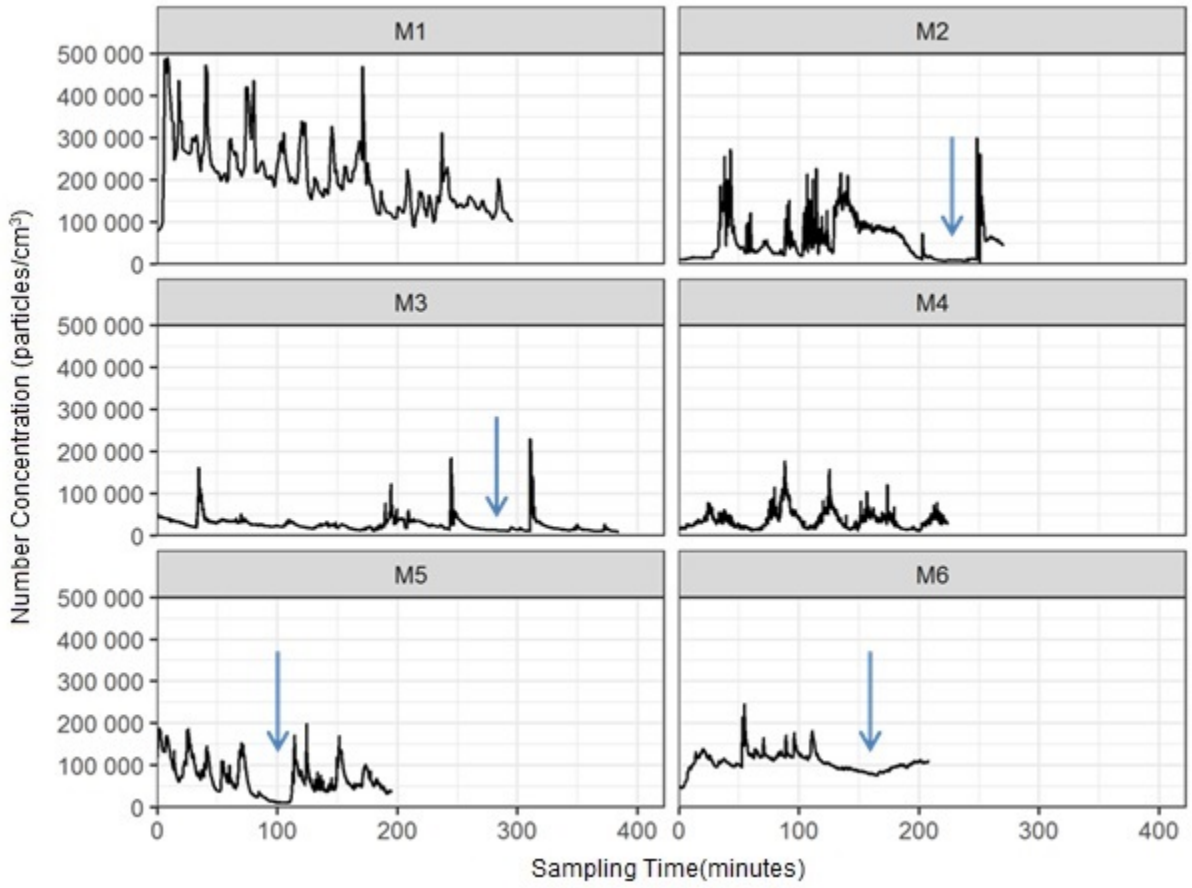

Figure 7. Typical daily profiles of number concentrations (particles/cm^3) measured with P-Trak®.

5.1.1.2 EEPS

The geometric means, geometric standard deviations, and the minima and maxima of the number concentrations measured with the EEPS are presented in Table 5 (note that the instrument could not be transported into M1 and M2). M4 and M6 show higher levels than M3 and M5; this is consistent with what was observed with the P-Trak®.

Figure 8 compares the number particle concentrations measured with the P-Trak® and the EEPS on the same sampling day. There is good agreement between the data from the two instruments; however, the CNCs (P-Trak®) appear to underestimate the concentrations compared to the EEPS, especially in M4 and M6, where higher contamination was observed.

Table 5. Descriptive statistics of instantaneous number concentrations measured using EEPS

Workplace	GM (particles/cm^3)	GSD	Min (particles/cm^3)	Max (particles/cm^3)
M3	30,000	1.71	10,300	217,000
M4	222,000	1.39	29,700	392,000
M5	60,100	1.58	33,500	305,000
M6	204,000	1.15	157,000	458,000

GM: geometric mean
GSD: geometric standard deviation
MIN: minimum; MAX: maximum

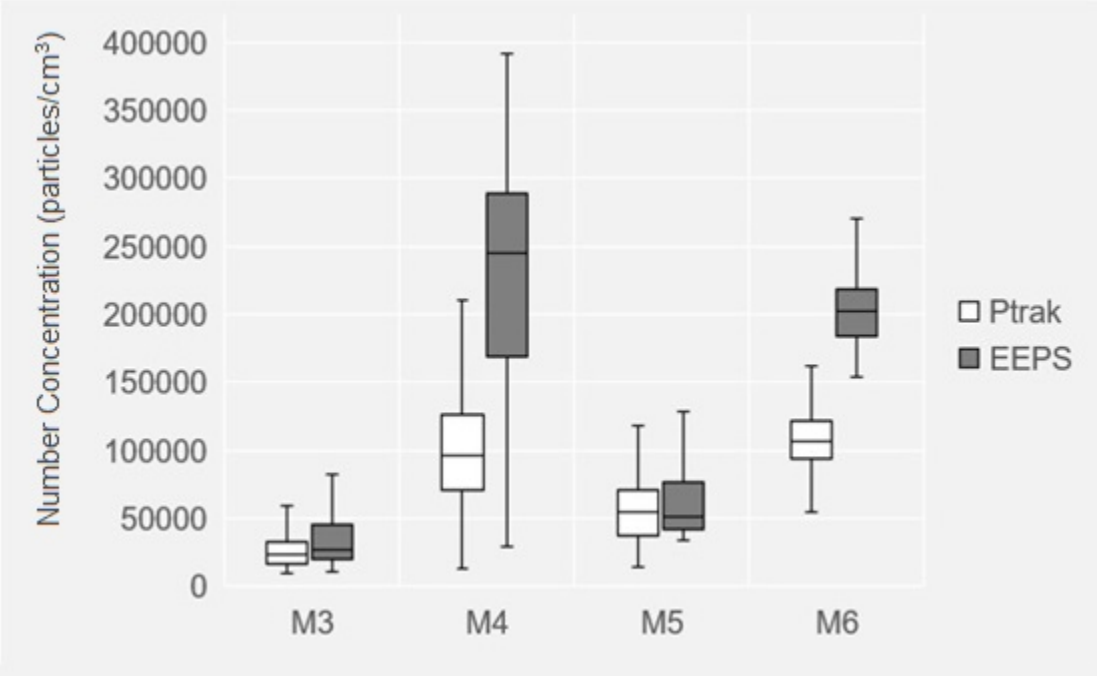

Figure 8. Comparison of number concentration distributions (particles/cm³) measured with P-Trak® and EEPS.

5.1.2 Particle size distributions of number concentrations (M3 to M6)

Figure 9 shows the particle size distributions of the number particle concentrations measured with the EEPS in workplaces M3 to M6. For M3, the two observed modes corresponded to electric mobility diameters of 22.1 nm and 107.5 nm. For M4 and M5, the main modes were 9.31 nm and 10.8 nm respectively, while the estimated main mode for M6 was 60.4 nm.

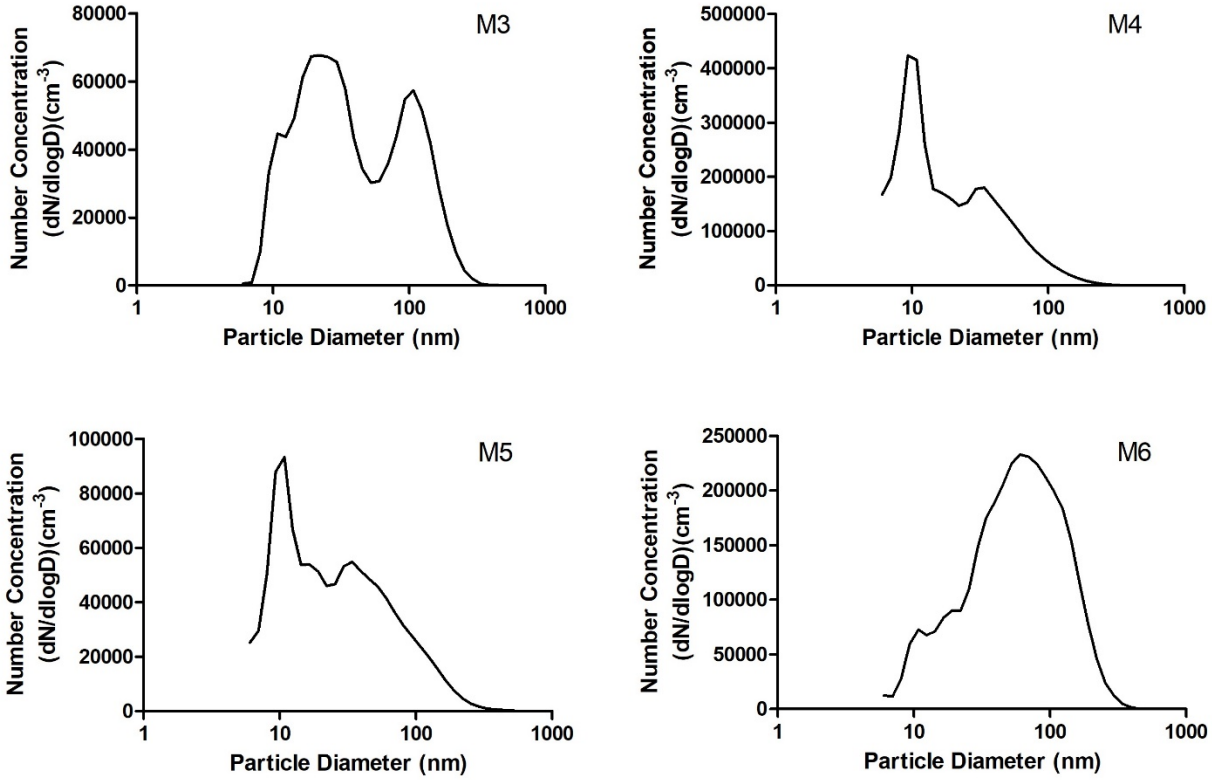

Figure 9. Mean particle size distributions of number particle concentrations measured with EEPS in workplaces M3 to M6.

Figure 10 shows the particle size distribution measured at M3 with the EEPS at the highest peak concentration. This peak (the main mode was then at 60.4 nm) can be traced to a truck entering near the instrument.

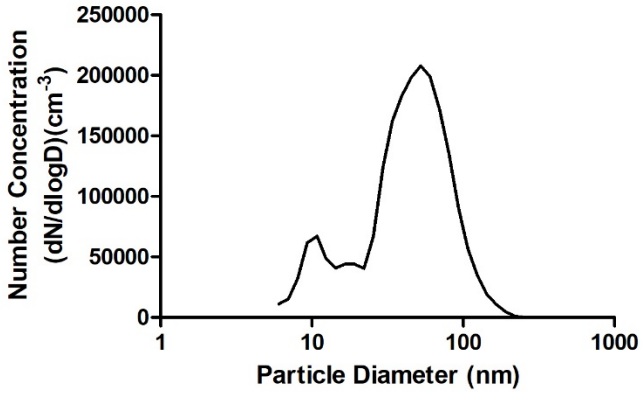

Figure 10. Particle size distribution of number particle concentrations measured with the EEPS at the main concentration peak at M3.

5.1.3 Mass concentrations

The geometric means, geometric standard deviations, minima and maxima of the daily mass concentrations measured at each workplace with the DustTrak™ 8520 and the DustTrak™ DRX are presented in tables 6 and 7, respectively.

Table 6. Descriptive statistics of daily mass concentrations measured with DustTrak™ 8520

Workplace	n	GM (mg/m^3)	GSD	Min (mg/m^3)	Max (mg/m^3)
M1 *	12	0.59	2.34	0.19	2.22
M2 *	12	0.05	1.93	0.02	0.15
M3 *	12	0.02	1.76	0.01	0.07
M4 **	12	0.16	2.09	0.04	0.42
M5 **	12	0.15	1.52	0.08	0.29
M6 **	12	1.10	1.39	0.65	1.69

n: number of daily averages
GM: geometric mean
GSD: geometric standard deviation
MIN: minimum; MAX: maximum
* The respirable fraction (PM_{Resp}) was assessed for M1, M2 and M3.
** The PM_{10} fraction was assessed for M4, M5 and M6.

Measurements taken with the DustTrak™ show a wide range of concentrations, with daily averages ranging from:

- 0.01 to 2.22 mg/m³ for PM_{Resp} fractions measured with the DustTrak™ 8520 (M1, M2 and M3)
- 0.04 to 1.69 mg/m³ for PM_{10} fractions measured with the DustTrak™ 8520 (M4, M5 and M6)
- 0.01 to 1.78 mg/m³ for PM_1 fractions measured with the DustTrak™ DRX
- 0.01 to 1.97 mg/m³ for $PM_{2.5}$ fractions measured with the DustTrak™ DRX
- 0.01 to 2.19 mg/m³ for PM_{Resp} fractions measured with the DustTrak™ DRX
- 0.01 to 3.22 mg/m³ for PM_{10} fractions measured with the DustTrak™ DRX

The two workplaces with the highest concentrations were the underground mine (M1) and the wax moulding shop (M6), with geometric mean concentrations of the PM_1 fraction of 0.50 mg/m³ and 0.84 mg/m³, respectively. The workplace with the lowest concentrations was the truck garage (M3) with a geometric mean concentration of 0.02 mg/m³ for the PM_1 fraction.

It should be noted that for all fractions, the highest daily concentrations measured with the DustTrak™ DRX were detected at M1 (Table 7). However, the highest daily mean concentration was measured at M6 with the same instrument, especially for the PM_1 fraction (Figure 11).

Table 7. Descriptive statistics of daily mass concentrations (mg/m³) measured with a DustTrak™ DRX

	PM_1				$PM_{2.5}$			PM_{Resp}			PM_{10}			PM_T		
Milieu	N	MG (ETG)	MIN	MAX	MG (ETG)	MIN	MAX	MG (ETG)	MIN	MAX	MG (ETG)	MIN	MAX	MG (ETG)	MIN	MAX
M1	11	0,50 (2,1)	0,2	1,78	0,56 (2,1)	0,21	1,97	0,61 (2,1)	0,22	2,19	0,72 (2,3)	0,24	3,22	0,77 (2,3)	0,24	3,48
M2	8	0,06 (1,8)	0,03	0,13	0,07 (1,8)	0,03	0,15	0,07 (1,9)	0,03	0,17	0,08 (1,9)	0,03	0,19	0,09 (1,9)	0,03	0,19
M3	12	0,02 (1,8)	0,01	0,05	0,02 (1,7)	0,01	0,05	0,03 (1,7)	0,01	0,06	0,03 (1,7)	0,01	0,06	0,03 (1,8)	0,01	0,07
M4	12	0,1 (2,1)	0,03	0,27	0,11 (2,1)	0,03	0,3	0,12 (2,1)	0,04	0,33	0,14 (2,1)	0,04	0,37	0,15 (2,1)	0,04	0,38
M5	12	0,08 (1,6)	0,05	0,16	0,09 (1,6)	0,05	0,2	0,11 (1,5)	0,06	0,22	0,13 (1,5)	0,07	0,26	0,14 (1,5)	0,07	0,28
M6	12	0,84 (1,4)	0,51	1,3	1,01 (1,4)	0,61	1,55	1,03 (1,4)	0,63	1,61	1,04 (1,4)	0,65	1,68	1,05 (1,4)	0,66	1,71

N: number of daily means; GM: geometric mean; GSD: geometric standard deviation; MIN: minimum; MAX: maximum

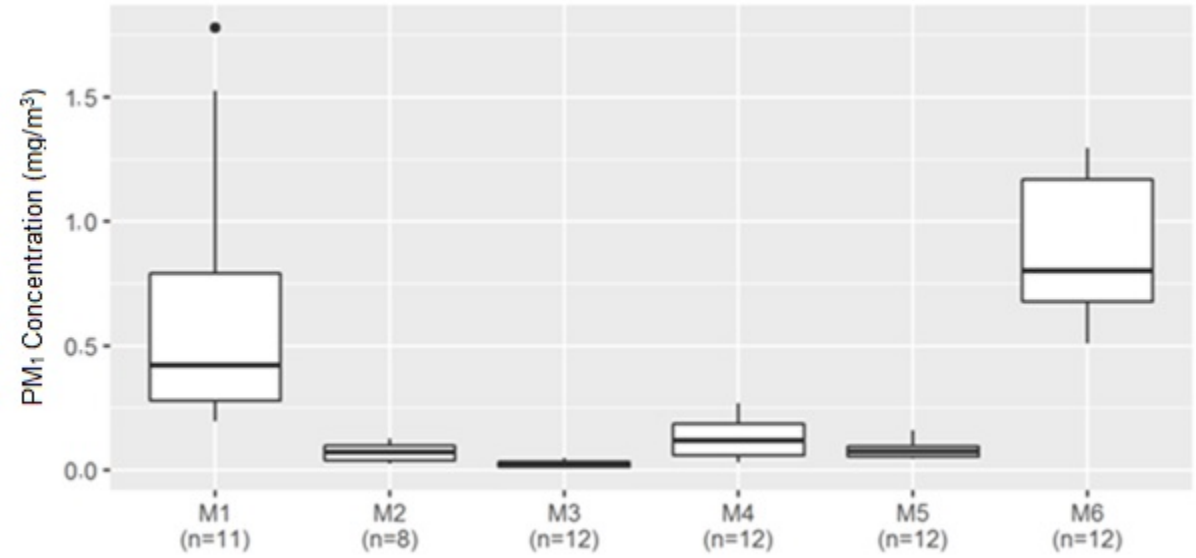

Figure 11. Distribution of daily mass concentrations (mg/m³) measured in the PM_1 fraction using a DustTrak™ DRX.

Figure 12 shows the distributions of instantaneous (averaged over 1 minute) mass concentrations measured for the PM_1 fraction with the DustTrak™ DRX in the six workplaces. Very high values (> 2.5 mg/m³) were measured at M1. As observed for the number concentrations measured with the P-Trak®, M6 can be seen to have a different profile from the other five workplaces, in the sense that its concentrations seem to be more homogeneous (less dispersion of measurements and the lowest GSD for the PM_1 fraction, at 1.4 mg/m³).

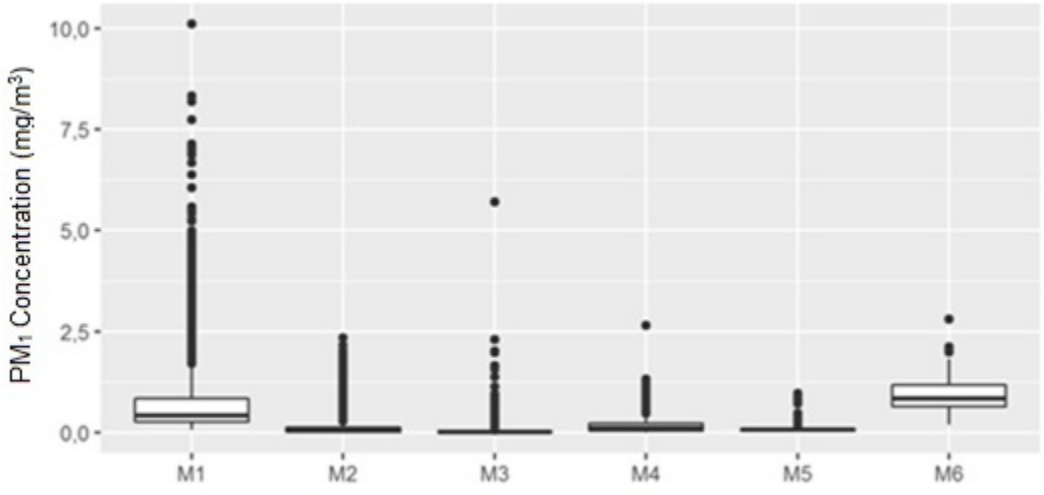

Figure 12. Distribution of instantaneous (averaged over 1 minute) mass concentrations (mg/m³) measured in the PM_1 fraction using the DustTrak™ DRX.

Based on the DustTrak™ DRX readings, the estimated mass concentrations measured in the PM_1 fractions represent, on average, 65% (M1), 67% (M2), 67% (M3), 67% (M4), 57% (M5) and 80% (M6) of the mass concentrations in the total fractions.

5.1.4 Concentrations of submicron elemental carbon EC_1 (M1, M2 and M3)

EC_1 was measured using Airtec devices in the environments where DEE was present. The geometric means, geometric standard deviations, minimum and maximum daily mass concentrations of EC are presented in Table 8. Figure 13 shows the mass concentration distributions of daily mean EC_1 concentrations in these three workplaces. The concentrations range from 0.004 to 0.148 mg/m³. M1 (underground mine) again stands out with the highest concentration level, while M3 (machine shop) again has the lowest contamination.

Table 8. Descriptive statistics of daily EC_1 mass concentrations measured with Airtecs in workplaces M1 to M3

Workplace	n	GM (mg/m^3)	GSD	Min (mg/m^3)	Max (mg/m^3)
M1	12	0.148	2.0	0.044	0.503
M2	12	0.025	2.8	0.003	0.120
M3	11	0.004	2.0	0.002	0.011

n: number of daily averages GM: geometric mean
GSD: geometric standard deviation MIN: minimum; MAX: maximum

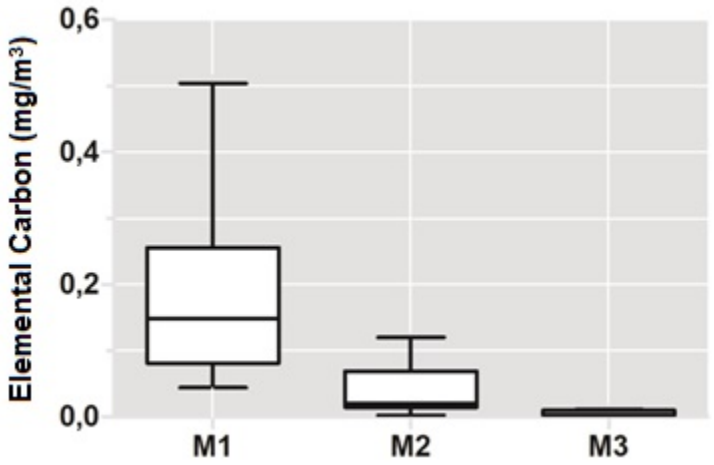

Figure 13. Distribution of daily EC_1 mass concentrations measured with Airtecs at M1, M2 and M3.

5.2 Time-averaged measurement

The following section presents the results of time-averaged measurement for each category of URNP, i.e. DEE (M1, M2 and M3), metal fumes and dusts (M4 and M5) and paraffin wax fumes (M6).

5.2.1 Diesel engine exhaust (DEE) (M1, M2 and M3)

The daily means, geometric standard deviations, and minimum and maximum time-averaged measurements of EC_R, TC_R, EC_1, TC_1, D_R and CD_R are presented in Table 9. Workplace M1 is characterized by higher concentrations compared to M2 and M3.

Table 9. Descriptive statistics of daily mass concentrations of EC_R, TC_R, EC_1, TC_1, D_R and CD_R in workplaces M1, M2 and M3

Parameter	Workplace	n	GM (mg/m^3)	GSD	Min (mg/m^3)	Max (mg/m^3)
	M1	11	0.137	2.3	0.037	0.580
EC_R	M2	12	0.025	2.4	0.008	0.072
	M3	12	0.003	2.4	<0.002	0.009
	M1	11	0.188	2.1	0.062	0.700
TC_R	M2	12	0.059	2.3	0.020	0.170
	M3	12	0.016	3.6	<0.003	0.054
	M1	12	0.133	2.3	0.033	0.510
EC_1	M2	12	0.015	2.2	0.006	0.055
	M3	12	0.002	2.0	<0.002	0.005
	M1	12	0.173	2.1	0.051	0.600
TC_1	M2	12	0.036	2.1	0.016	0.110
	M3	12	0.010	3.3	<0.003	0.039
	M1	11	0.530	2.2	0.260	3.30
D_R	M2	11	0.061	2.6	<0.023	0.340
	M3	12	0.036	1.5	0.018	0.062
	M1	9	0.244	1.9	0.080	1.00
CD_R	M2	11	0.100	2.5	0.040	0.470
	M3	12	0.019	1.7	<0.015	0.045

n: number of daily averages
GM: geometric mean
GSD: geometric standard deviation

MIN: minimum; MAX: maximum

Table 10 shows the ratios TC_R/EC_R, TC_1/EC_1, TC_1/TC_R, EC_1/EC_R and CD_R/D_R for the three workplaces. The higher the TC/EC ratios, the more organic carbon there is in the total carbon measurement. TC/EC ratios greater than 2 were calculated for M2 and M3, indicating that other sources of organic carbon are present and contribute significantly to total carbon concentrations. On the other hand, ratios of 1.30 and 1.37 were obtained for M1.

The higher the TC_1/TC_R or EC_1/EC_R ratio, the more carbon is present in the submicron fraction. The elemental carbons in the submicron fraction (EC_1) for M1 account for 97% of those in the respirable fraction (EC_R). Only 60% of the carbon in M2 and 67% of the carbon in M3 appears to be submicron in size. Similar results were obtained for total carbon. This indicates that the carbon aerosol in workplace M1 is finer and that the submicron fraction occupies a greater proportion.

Table 10. Calculated ratios between the different concentration estimators

	M1	M2	M3
TC_R/EC_R	1.37	2.36	5.33
TC_1/EC_1	1.30	2.40	5.00
TC_1/TC_R	0.92	0.61	0.63
EC_1/EC_R	0.97	0.60	0.67
CD_R/D_R	0.46	0.61	0.53

The higher the CD_R/D_R ratio, the more combustible dust is in the respirable fraction. This ratio was established at 46% for M1 and slightly higher for M2 and M3, indicating the presence of non-combustible dust sources other than DEE in all three workplaces, but more specifically in M1, where the majority of aerosols are found in the non-combustible fraction.

5.2.2 Metal dust and fumes (M4 and M5)

5.2.2.1 Mass concentrations of metal dust and fumes

The mass concentrations of total dust (37-mm cassettes) and fine and ultrafine particles (Sioutas, <10 µm) were measured at M4 and M5. The average concentrations are reported in Table 11. Concentrations in M5 appear to be higher than those in M4 for both sampling devices. The mean concentrations measured with the Sioutas impactor were 28% and 55% lower, respectively, than those obtained with the 37-mm cassettes at M4 and M5.

Figure 14 shows the relationship between the measurements made with the two types of samplers (37-mm cassette and Sioutas impactor). A good correlation is obtained, but the 0.3 slope of the regression line confirms that the Sioutas concentrations were lower than those of the 37-mm cassettes.

Table 11. Descriptive statistics of daily mass concentrations of fumes and metal dust, measured with 37-mm cassettes or Sioutas impactors in workplaces M4 and M5

Workplace	Instrument	n	GM (mg/m^3)	GSD	Min (mg/m^3)	Max (mg/m^3)
M4	Cassette	12	0.188	3.3	<0.080	1.20
	Impactor	12	0.135	2.3	0.036	0.56
M5	Cassette	12	0.321	1.9	<0.074	0.92
	Impactor	11	0.145	3.0	0.009	0.38

n: number of samples;
GM: geometric mean
GSD: geometric standard deviation
MIN: minimum; MAX: maximum

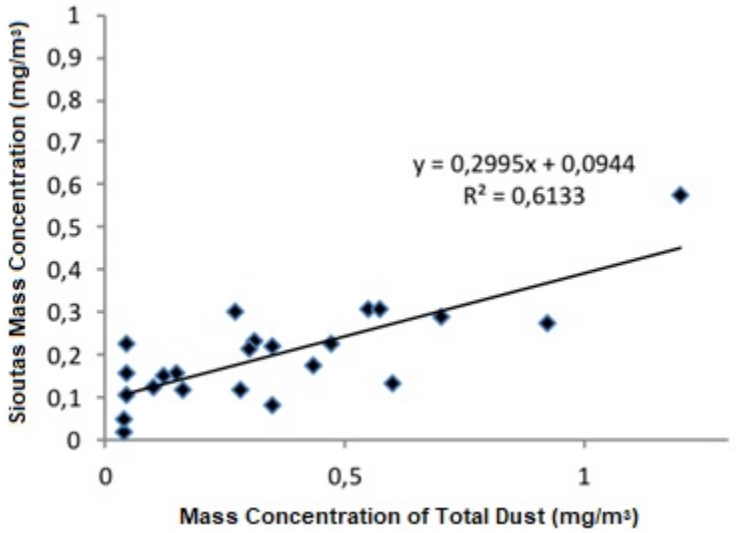

Figure 14. Correlation between mass concentrations measured with 37-mm cassettes and Sioutas impactors in workplaces M4 and M5.

Table 12 presents the distributions of mass concentrations over each of the impactor stages in workplaces M4 and M5, as well as the MMAD calculated for each workplace. For M4 and M5, 51% of the dust mass was collected on the first impactor stage (i.e. between 2.5 and 10 µm). A MMAD of 1.8 µm was calculated for M4 and 2 µm for M5.

Table 12. Mean distribution (%) of mass concentrations of particles on various impactor stages, and MMAD values for M4 and M5

	M4 (n=12)	M5 (n=11)
2.5–10 µm	51	51
1.0–2.5 µm	19	23
0.5–1.0 µm	11	10
0.25–0.5 µm	19	16
<0.25 µm	–	–
MMAD (µm)	1.8	2.0

n: number of samples;
MMAD: Mass median aerodynamic diameter

5.2.2.2 Metal concentrations

Of all the metals measured, only chromium, cobalt, copper, iron, manganese, nickel, lead, vanadium and zinc were identified at M4 and/or M5 in the inhalable dust (IOM cassette), total dust (37-mm cassettes), and fine and ultrafine particles (Sioutas, <10 µm) (Table 13). Aluminum, cadmium and magnesium were not detected and are therefore not covered in this section.

At M4, iron, copper, manganese and lead were found in almost every sample. Zinc was also very prevalent, but mainly on the last impactor stages. Occasional occurrences of iron, cobalt and chromium were also observed. Nickel was not measured at this workplace.

At M5, copper, iron and chromium occurred very frequently. There were also occasional occurrences of manganese, cobalt, and nickel. Lead and zinc, both substantially present at M4, were not detected at M5, nor was vanadium.

Table 13 presents the metal concentrations measured in each workplace. Concentrations are reported when at least one sample contained the element. Whereas the choice of sampling device had little effect on concentrations in the case of M4, significant differences were observed for M5. There, the 37-mm cassettes yielded metal concentrations that were, on average, 30% lower than those measured with the IOMs, while the concentrations measured with the Sioutas impactors averaged 50% lower. These results suggest that the particles collected from M5 (machining) are coarser than those from M4 (foundry).

Table 13. Descriptive statistics of daily mean concentrations of metals measured with IOM cassettes, 37-mm cassettes and Sioutas impactors at M4 and M5

		M4				M5			
		GM (µg/m3)	GSD	Min (µg/m3)	Max (µg/m3)	GM (µg/m3)	GSD	Min (µg/m^3)	Max (µg/m^3)
Chromium	**IOM**	1.73	1.2	<2.2	2.8	24.3	1.6	11	45
	37 mm	N.D.	–	–	–	11.2	2.2	3.4	38
	Sioutas	2.1	1.3	<1.8	2.7	4.0	1.6	2.3	10.5
Cobalt	**IOM**	0.09	1.6	<0.09	0.2	0.11	1.6	<0.1	0.24
	37 mm	0.09	1.1	<0.11	0.1	0.10	1.4	<0.11	0.20
	Sioutas	0.10	1.3	<0.04	0.1	0.10	1.3	<0.04	0.13
Copper	**IOM**	4.3	2.3	<1.0	8.8	5.9	2.5	1.7	24
	37 mm	3.5	2.1	<1.3	8.0	3.4	2.4	<1.3	21
	Sioutas	3.4	2.0	1.4	8.3	2.6	2.2	1.2	15
Iron	**IOM**	23.9	1.6	<22.3	52	225	1.7	110	510
	37 mm	23.1	1.2	<29.8	34	124	2.3	40	490
	Sioutas	22.6	1.5	<9.7	49	50	1.8	25	170
Manganese	**IOM**	10.8	2.3	<2.4	26	2.8	2.0	<2.4	9.9
	37 mm	10.4	1.6	5.8	25	2.9	1.6	<3.1	9.3
	Sioutas	9.0	1.8	<3	23	2.2	1.4	<1.8	4.7
Nickel	**IOM**	N.D.	–	–	–	7.3	1.8	<4.9	16
	37 mm	N.D.	–	–	–	5.3	1.5	<5.7	15
	Sioutas	N.D.	–	–	–	4.2	1.3	<2.4	7.2
Lead	**IOM**	0.6	2.0	<0.2	1.4	N.D.	–	–	–
	37 mm	0.6	1.6	<0.3	1.2	N.D.	–	–	–
	Sioutas	0.5	1.5	<0.3	1	N.D.	–	–	–
Vanadium	**IOM**	N.D.	–	–	–	N.D.	–	–	–
	37 mm	N.D.	–	–	–	N.D.	–	–	–
	Sioutas	0.2	1.4	<0.1	0.3	N.D.	–	–	–
Zinc	**IOM**	2.1	1.5	<2.2	4.6	N.D.	–	–	–
	37 mm	2.8	1.6	<3.0	7	N.D.	–	–	–
	Sioutas	2.9	1.6	<1	5.6	2.1	1.3	<1.2	3

IOM: N=10 for M4 and N=8 for M5
37 mm: N=12 for M4 and N=12 for M5
Sioutas: N=12 for M4 and N=11 for M5
N.D.: Not detected

The characterization can be refined through a detailed analysis of the metals deposited on the different impactor stages (Table 14). MMAD values were seen to vary depending on the workplace and the type of metal. At M4, all MMADs remained below 1 µm regardless of the metal. At M5, the MMADs were higher; for example, the values for chromium, cobalt, iron and nickel were 1 µm or greater.

Table 14. Mean distribution (%) of metal concentrations deposited on various impactor stages, and MMAD values for M4 and M5

	Chromium	Cobalt	Copper	Iron	Manganese	Nickel	Lead	Vanadium	Zinc
M4	n=2	n=2	n=12	n=3	n=11	n=0	n=11	n=3	n=8
2.5–10 µm	18	28	6	24	4	–	24	17	16
1.0–2.5 µm	18	18	7	15	4	–	10	17	13
0.5–1.0 µm	18	18	8	31	7	–	9	17	13
0.25–0.5 µm	22	18	30	15	48	–	17	17	20
<0.25 µm	22	18	49	15	37	–	39	33	37
MMAD (µm)	0.7	0.9	0.2	0.9	0.3	–	0.6	0.5	0.4
M5	n=11	n=2	n=11	n=11	n=3	n=2	n=0	n=0	n=1
2.5–10 µm	44	31	13	46	29	31	–	–	18
1.0–2.5 µm	15	17	8	19	15	16	–	–	18
0.5–1.0 µm	11	17	8	10	15	16	–	–	18
0.25–0.5 µm	12	17	9	10	20	16	–	–	18
<0.25 µm	18	17	63	14	22	20	–	–	26
								–	
MMAD (µm)	2.2	1	0.2	2.4	0.9	1	–	–	0.6

n: number of samples;
MMAD: Mass median aerodynamic diameter

5.2.3 Paraffin wax fumes

A concentration of 0.2 mg/m^3 was measured in the wax workshop with a 37-mm cassette. The other seven measurements made with these cassettes all remained below the limit of quantification, with concentrations of less than 0.2 mg/m^3. Ten measurements were then performed with the impactors and yielded a geometric mean concentration of 0.15 mg/m^3, with levels ranging from 0.07 to 0.37 mg/m^3.

Table 15 shows the mean distribution of paraffin wax concentrations on the different impactor stages, and the MMAD of particles captured at M6. It can be seen that 51% of the particles in the impactor were deposited on stages smaller than 0.5 µm, and that the MMAD was 0.8 µm.

Table 15. Mean distribution (%) of paraffin wax concentrations on various impactor stages, and MMAD value for M6

	M6 (n=10)
2.5–10 µm	20
1.0–2.5 µm	15
0.5–1.0 µm	16
0.25–0.5 µm	28
<0.25 µm	23
MMAD (µm)	0.8

n: number of samples;
MMAD: Mass median aerodynamic diameter

5.3 Microscopy analysis

Nearly 1,300 particles or particle agglomerates were analyzed: 60 in M1, 20 in M2, 20 in M3, 419 in M4, 409 in M5 and 360 in M6. Each analysis included a particle image and an EDS analysis.

5.3.1 Mine (M1)

Figure 15 shows a sample image of the hole in one of the grids sampled at M1. The particles identified here were essentially spherical carbon particles about 10 nanometers in size, agglomerated in a long chain. Figure 16 gives an overview of this type of particle, which was observed in abundance. Fine silica particles several hundred nanometres in size (Figure 17, left) and highly agglomerated metallic particles (Figure 17, right) were also identified at the mine. The metallic particles were found to consist mainly of iron, manganese and zinc.

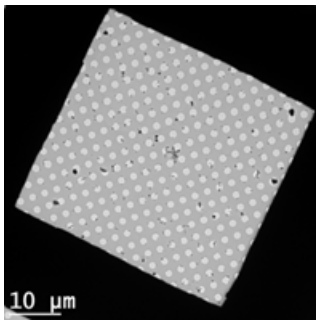

Figure 15. TEM bright-field image (400X) of a hole in a grid used for particle sampling at M1.

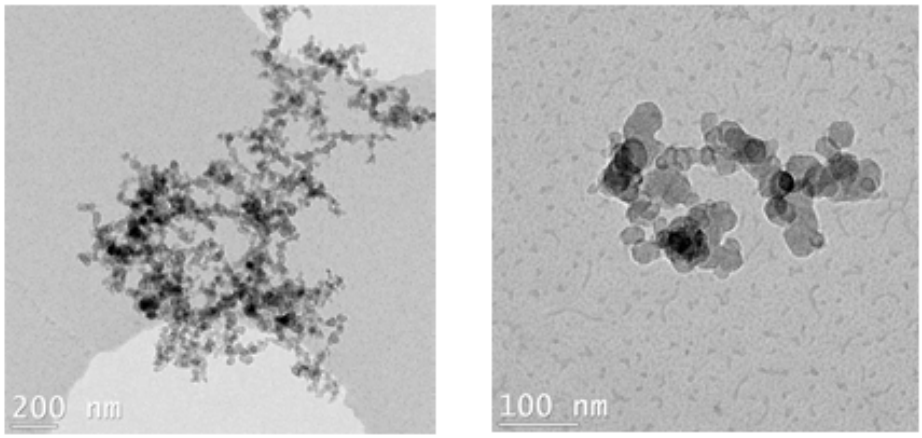

Figure 16. Examples of TEM bright-field images of the type of carbon particles predominantly identified at M1.

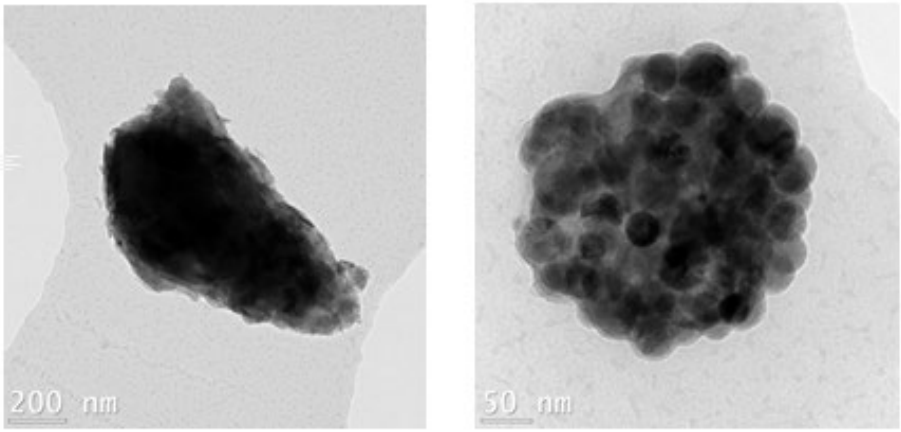

Figure 17. Examples of TEM bright-field images of particles identified at M1.

5.3.2 Underground environment and mechanical workshop (M2 and M3)

M2 and M3 are discussed in the same section, since the diesel exhaust particulate matter had the same characteristics. Figure 18 shows an example of an image of a hole in one of the grids exposed at M2 and M3. The particles identified are essentially spherical carbon particles about 10 nanometers in size, agglomerated in a long chain. Figure 19 gives an overview of this type of particle. Salt particles (NaCl) in the micrometre range were also identified at M3 (Figure 20, left). Spots were observed on the grids at M2 and M3. These spots are associated with liquid aerosols composed of carbonaceous elements (Figure 20, right).

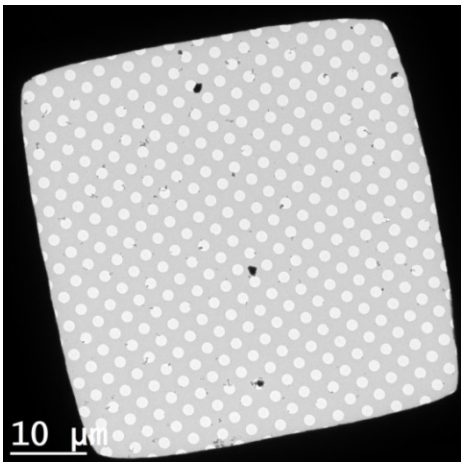

Figure 18. TEM bright-field image (400X) of a hole in a grid used for particle sampling at M2 (subsurface workplace).

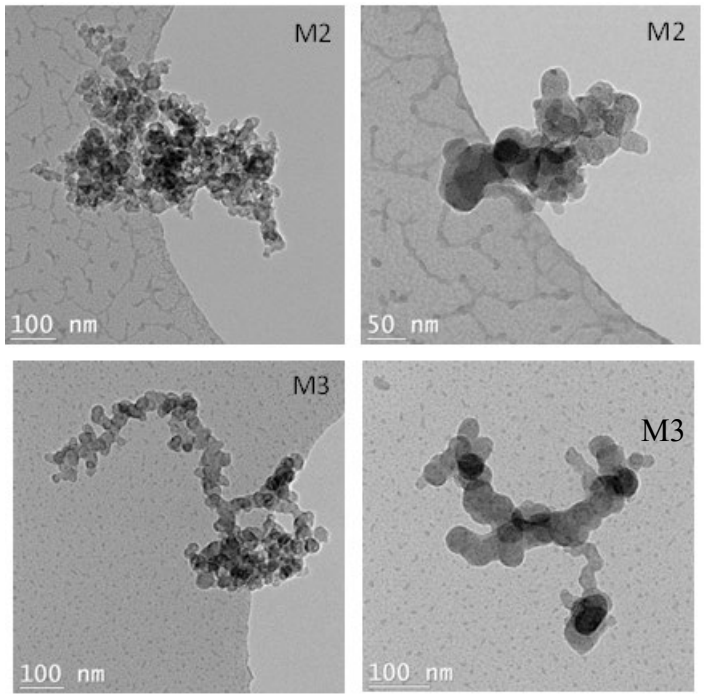

Figure 19. Examples of TEM bright-field images of the type of carbon particle predominantly identified at M2 and M3.

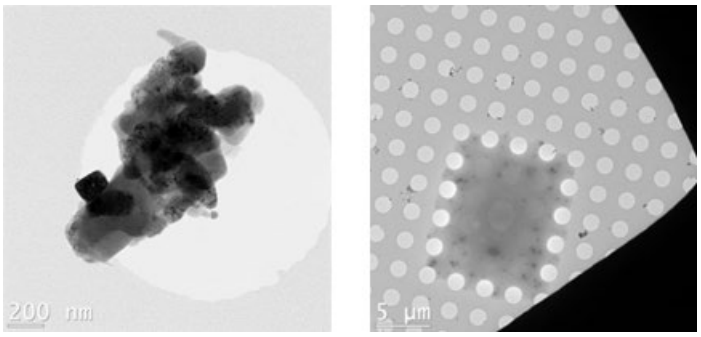

Figure 20. Examples of TEM bright-field images of particles identified at M2 or M3.

5.3.3 Foundry (M4)

Figure 21 shows a sample image of a hole in a grid exposed at M4. The particles identified at the foundry were essentially spherical fragments ranging from 50 to 500 nm, isolated or in agglomerates of up to about 10 particles, composed mostly and quite consistently of metal oxides. Figure 22 provides an overview of this type of particle, which is quite abundant, accounting for 52% of the particles analyzed. The following elements were identified, in descending order of frequency: iron (in 66% of the particles analyzed), chromium (64%), silicon (61%), manganese (59%), zinc (29%), copper (22%), aluminum (9%), nickel (8%) and lead (8%).

Other types of particles were also detected; illustrations are provided in Figure 23. They include long-chain nanoparticles similar to those observed at M5 (see subsection 5.3.4), needle-shaped zinc oxides about 500 nm long, and coarser metal particles of micrometre size and non-spherical shape.

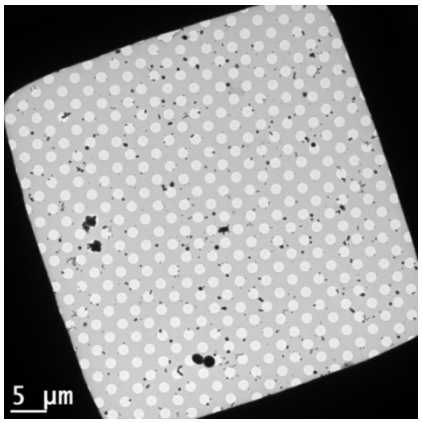

Figure 21. TEM bright-field image (400X) of a hole in a grid used for particle sampling at M4 (foundry).

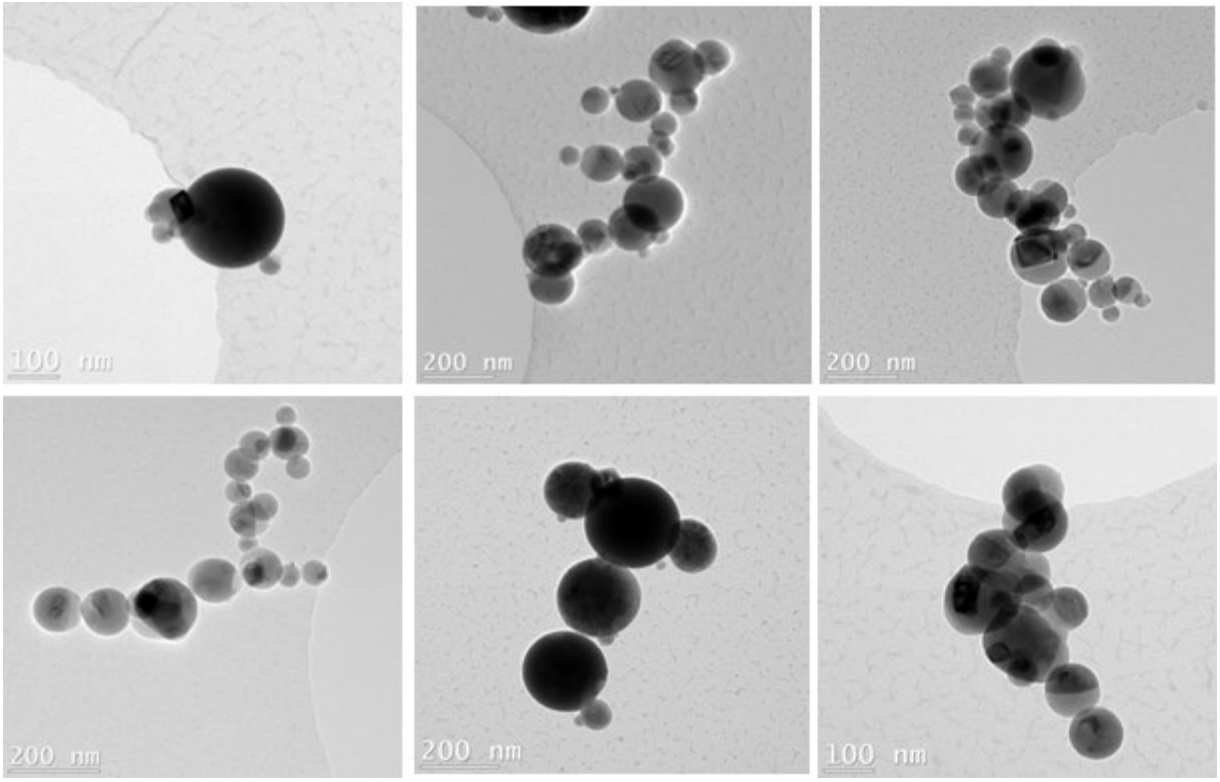

Figure 22. Examples of TEM bright-field images of the type of particle predominantly identified at M4.

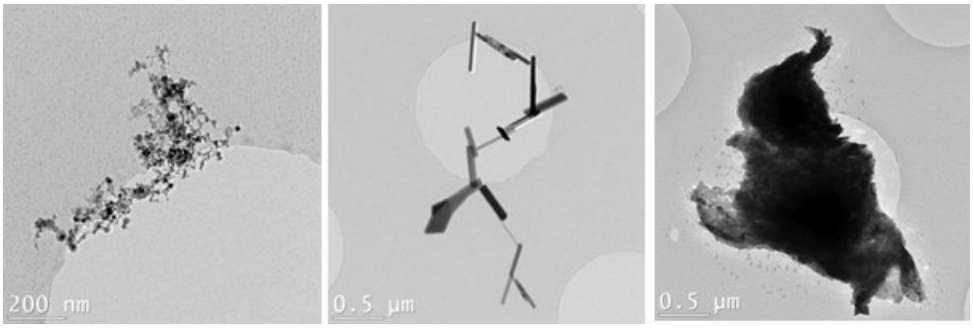

Figure 23. Examples of TEM bright-field images of particles identified at M4.

5.3.4 Machine shop (M5)

Figure 24 and Figure 25 show sample images of holes in grids exposed near an arc cutting station and a grinding station at M5.

The particles identified at M5 were of various shapes and compositions. The following elements were found, in order of frequency: iron (in 77% of the particles analyzed), chromium (48%), silicon (41%), manganese (35%), nickel (28%), aluminum (26%), copper (13%), zinc (8%), and lead (3%).

There were two main types of particles. The first category consisted of very fine particles, on the order of a few nanometres, highly agglomerated and chain-shaped (Figure 26). These particles were detected mainly on sample grids taken near TIG welding and arc cutting areas. The agglomerates can reach sizes in the micrometre range. These particles contain mainly iron, copper, silicon, chromium, manganese, nickel and, more rarely, potassium, sulphur, phosphorus and chlorine. The second category, illustrated in Figure 27, consisted of particles of various shapes, non-specific or non-spherical, rather coarse (0.5 to 5 µm) and with various chemical compositions. They were mainly found on sample grids taken near grinding operations. These particles contain mainly iron, aluminum, silicon, chromium, nickel, manganese, titanium and, more rarely niobium, potassium and zirconium.

In addition, spherical metal oxide particles similar in morphology and composition to those previously presented in M4 (Figure 22) were also observed on a few occasions, along with carbon particles of various shapes, similar to those described later in section 5.3.5 for M6.

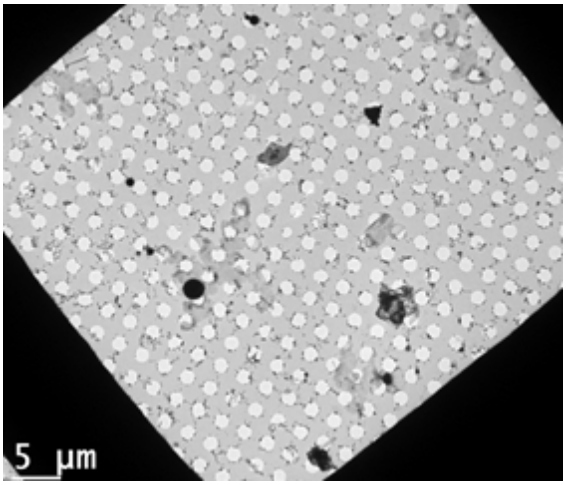

Figure 24. TEM bright-field image (400X) of a hole in a grid used for particle sampling at M5 (machine shop) near the arc cutting station.

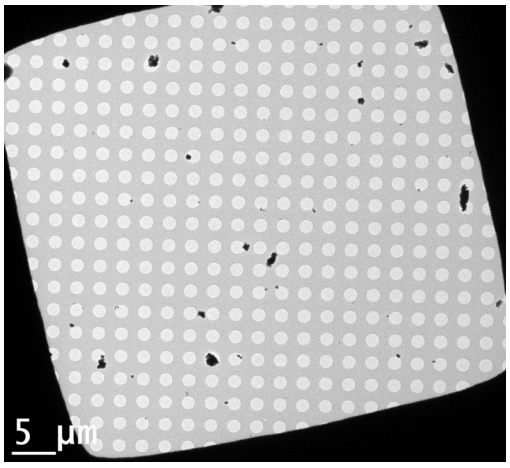

Figure 25. TEM bright-field image (400X) of a hole in a grid used for particle sampling in a grinding area at M5 (machine shop).

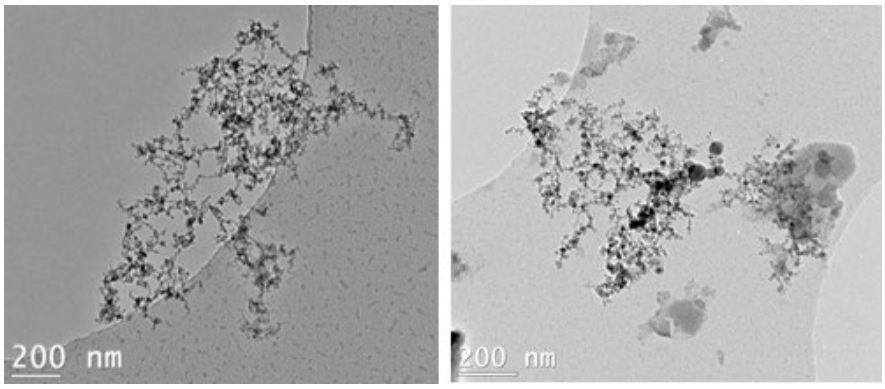

Figure 26. Examples of TEM bright-field images (400X) of particles identified near the arc cutting station at M5.

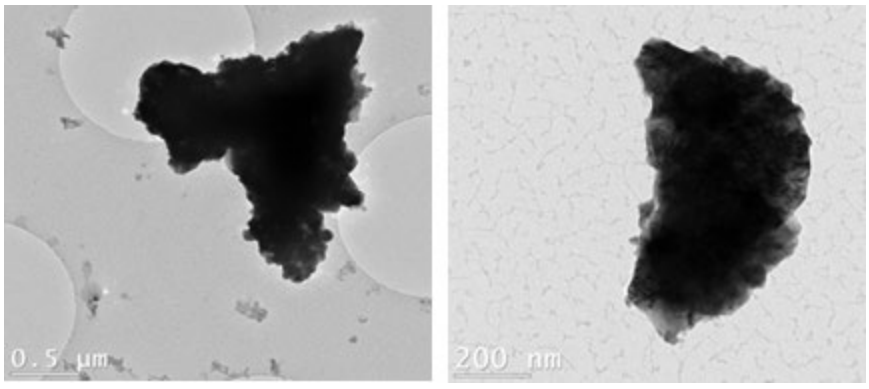

Figure 27. Examples of TEM bright-field images (400X) of particles identified near the grinding shop at M5.

5.3.5 Paraffin wax workshop (M6)

Figure 28 shows a sample image of a hole in a grid exposed at M6. The particles identified here were carbon-rich, very homogeneous and of various shapes ranging from rather spherical to rod-shaped, as shown in Figure 29. They ranged in size from a few hundred nanometres to a few micrometres, and make up 65% of the particles observed in this workplace. Particles similar to those shown in Figure 26 were also identified at M6.

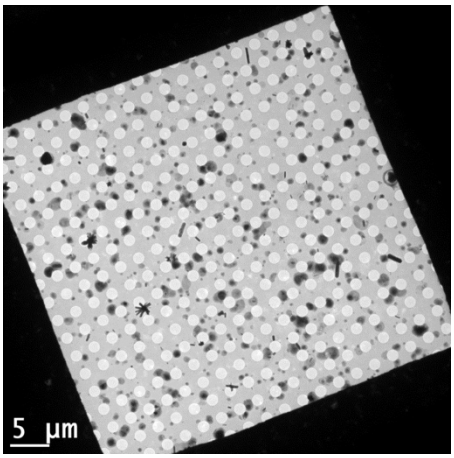

Figure 28. TEM bright-field image (400X) of a hole in a grid used to collect particles at M6 (wax casting shop).

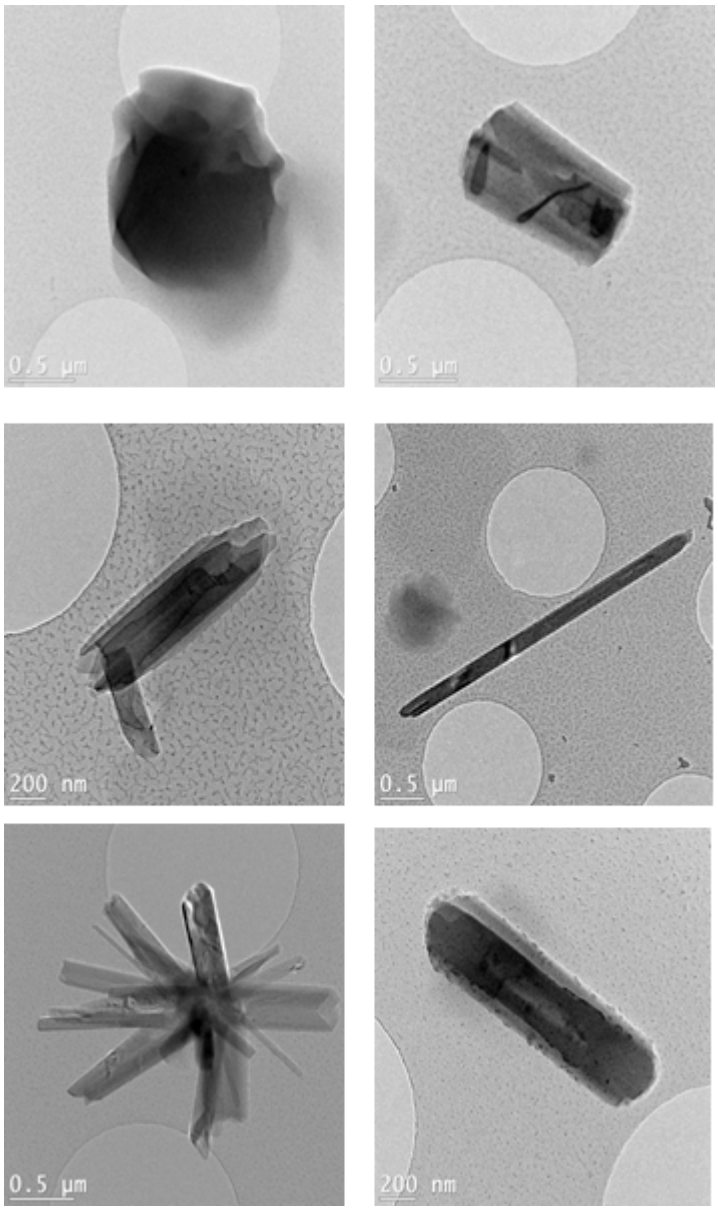

Figure 29. Examples of TEM bright-field images (400X) of particles identified at M6 (wax casting shop).

5.4 Comparison of different exposure indicators

5.4.1 Diesel engine exhaust (M1, M2 and M3)

Strong correlations were obtained between the time-averaged measurements of elemental carbon (EC_1 and EC_R) and those obtained with DRIs (Table 16). This shows that, overall, the concentrations indicated by the DRIs increase when EC_1 and EC_R concentrations rise. For the time-averaged EC_1 measurements, the best correlations were obtained first with the concentrations estimated using the Airtec (r=0.97), then with PM_{Resp} and PM_1 as measured by the

DustTrak™ DRX (r=0.94 in both cases), and finally with those estimated by the DustTrak™ 8520 (r=0.91) and the P-Trak® (r=0.86). For time-averaged EC_R measurements, the strongest correlation was with data from the DustTrak™ 8520 (r=0.90). It can be seen that the strength of correlations between measurements with the same instrument varies from one workplace to the next. For example, at M2, correlations were very strong for the DustTrak™ DRX and weaker with the Airtec data. The situation is reversed at M1, with the Airtec data showing very strong correlations and the DustTrak™ DRX data showing weaker correlations.

Table 16. Spearman's correlation coefficients between EC concentrations measured in the submicron (EC_1) and respirable (EC_R) fractions (time-averaged measurements) and the daily averages of parameters measured with the different DRIs used at M1, M2 and M3

	EC_1 concentrations (time-averaged)					**EC_R concentrations (time-averaged)**				
	P-Trak®[a]	**DustTrak™ DRX[b]**	**DustTrak™ DRX[c]**	**DustTrak™8520[c]**	**Airtec[d]**	**P-Trak®[a]**	**DustTrak™ DRX[b]**	**DustTrak™ DRX[c]**	**DustTrak™ 8520c**	**Airtec[d]**
		PM_1	PM_{Resp}	PM_{Resp}	EC_1		PM_1	PM_{Resp}	PM_{Resp}	EC_1
M1 ***n=12***	0.60**	0.46*	0.42*	0.65**	0.96***	0.63***	0.43*	0.37	0.68**	0.97***
M2 ***n=12***	0.67*	0.98***	0.90**	0.88**	0.73**	0.88**	0.79*	0.76*	0.79**	0.54
M3 ***n=12***	0.75**	0.70*	0.73**	0.68*	0.74**	0.67*	0.52	.0.55	0.50	0.65*
All ***n=36***	0.86***	0.94***	0.94***	0.91***	0.97***	0.87***	0.86***	0.87***	0.90***	0.89***

[a] number concentration; [b] mass concentration in the submicron fraction (PM_1); [c] mass concentration in the respirable fraction (PM_{Resp}); [d] concentration of elemental carbon in the submicron fraction.
*p<0.05; **p<0.01; ***p<0.001

Figure 30 shows the relationships between the different indicators obtained with DRIs (P-Trak®, DustTrak™ 8520, Airtec) at M2 and M3 in relation to M1 (100%), in comparison with the time-averaged EC_R and EC_1 measurements. It can be seen that the EC_1 proportions (daily averages) obtained with the Airtec were very similar to the time-averaged measurements of EC_R and EC_1. The data from the P-Trak® were different, with proportionally higher concentrations for M2 and M3 than for the other indicators.

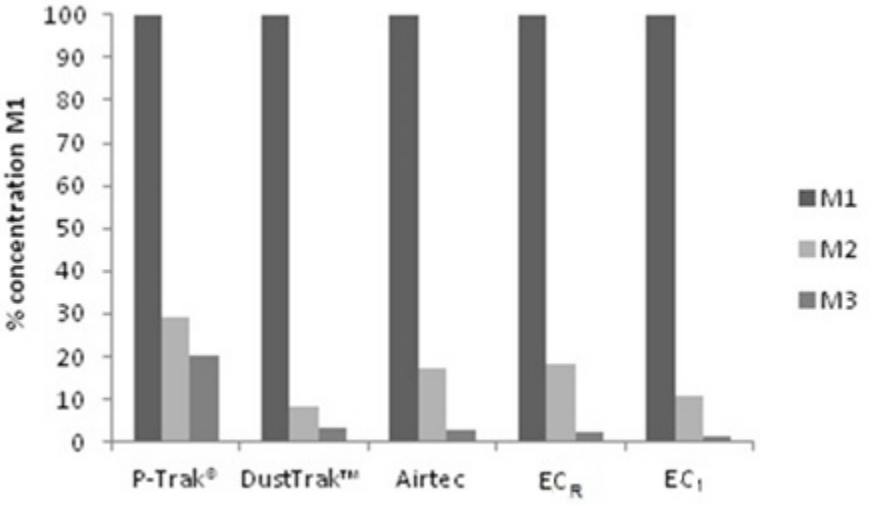

Figure 30. Proportion of concentrations measured by DRIs at M2 and M3, relative to M1.

Figure 31 shows the correlation between the time-averaged EC_R measurements and the daily averages of the recorded mass concentrations, also in the respirable fraction, with the DustTrak™ 8520. Figure 32 shows the correlation between the EC_1 concentrations estimated according to the time-averaged approach and those recorded with the Airtecs.

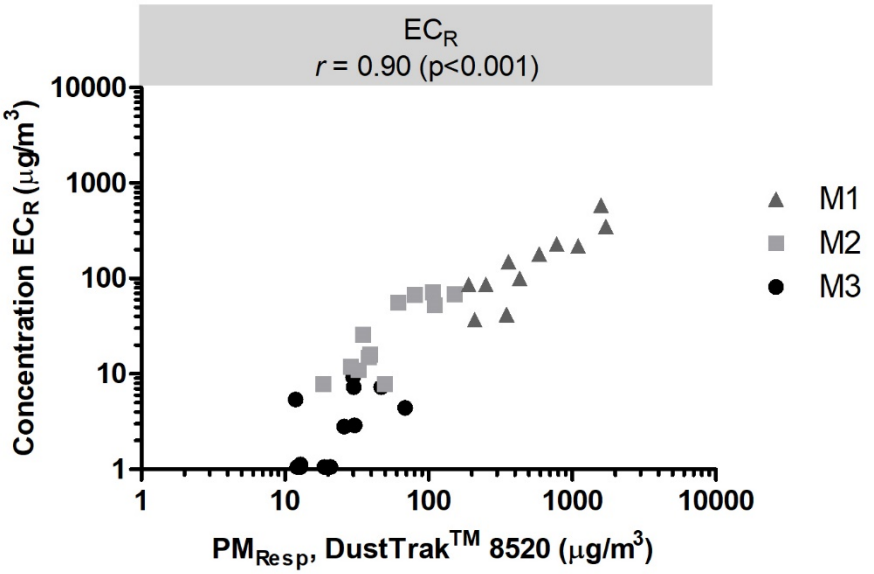

Figure 31. Correlation between time-averaged measurements of respirable elemental carbon (EC_R) and daily averages of measurements recorded with DustTrak™ 8520 for the respirable fraction (PM_{Resp}) at M1, M2 and M3.

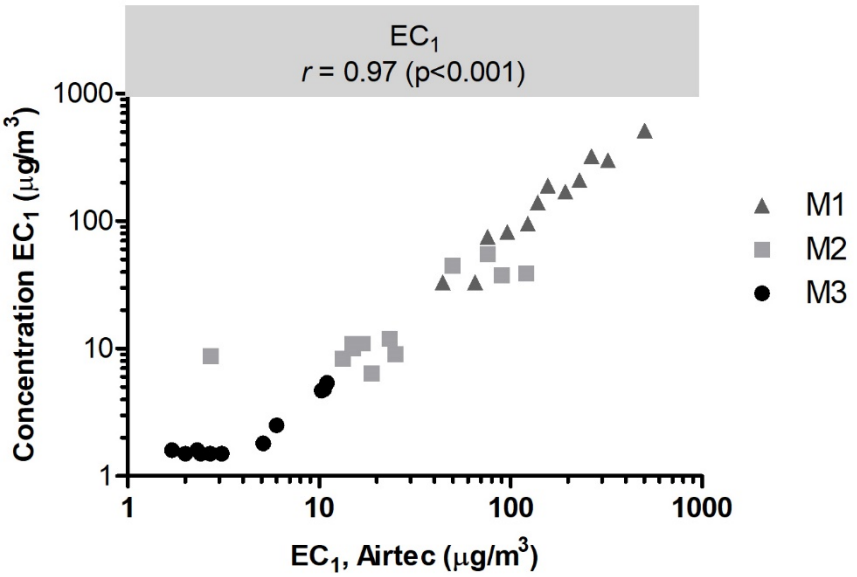

Figure 32. Correlation between time-averaged measurements of elemental carbon in the submicron fraction (EC_1) and daily averages recorded with Airtecs at M1, M2 and M3.

Although significant correlations were observed (Table 16), the levels measured by DRIs may vary quantitatively. The average ratios between daily EC_R concentrations and those estimated with the DustTrak™ 8520 therefore vary widely from one workplace to the next. They are as follows: 0.20 for M1, 0.55 for M2 and 0.16 for M3. These results indicate that a correction should be made to the measurements recorded by DustTrak™ 8520 to quantitatively estimate EC_R levels. Equation (1) presents the linear regression, for the three workplaces (M1 to M3), between the time-averaged EC_R measurements and the mean daily concentrations estimated with the DustTrak™ 8520 (R=0.9; p<0.01).

$$EC_R\ (\mu g/m3) = 0.16 \times [\text{DustTrak™ 8520 (expressed in } \mu g/m^3)] + 17.5 \quad (1)$$

Equation (2) is the linear regression between the time-averaged EC_R measurements and the mean daily number concentrations measured with the P-Trak® (R=0.88; p<0.01).

$$EC_R\ (\mu g/m3) = 0.0014 \times [\text{P-Trak® (expressed as particles/cm}^3)] - 11.7 \quad (2)$$

Finally, it should be noted that the correlation obtained between the time-averaged EC_1 measurements and the estimated mean daily concentrations from the Airtecs is the highest obtained (R=0.97; p<0.01). Furthermore, the ratio between the concentrations obtained from time-averaged measurements and Airtec measurements is 1.01, indicating a similar range. Equation (3) shows the linear relationship between these two measures of EC_1.

$$EC_1\ (\mu g/m3) = 1.01 \times [\text{Airtec } (\mu g/m^3)] - 9.4 \quad (3)$$

5.4.2 Metal fumes (M4 and M5)

With regard to total dust levels at M4, there were good correlations between the time-averaged measurements made with 37-mm cassettes and impactors, and the results obtained with DRIs (Table 17 and Table 18). For M5, however, only the measurements made with 37-mm cassettes were correlated with DRI results.

Table 17. Total dust concentration (D_T) – Spearman's correlation coefficients between time-averaged measurements (37-mm cassettes) and daily averages measured with DRIs

	D_T 37 mm						
	P-Trak®[a]	**DustTrak™ DRX[b]**					**DustTrak™ 8520[b]**
		PM_1	$PM_{2.5}$	PM_{Resp}	PM_{10}	PM_{Tot}	PM_{10}
M4 *n=12*	0.58*	0.70*	0.71**	0.72**	0.73**	0.73**	0.72**
M5 *n=12*	0.77**	0.75**	0.71**	0.70*	0.61*	0.60*	0.75**
All *n=24*	0.54**	0.59**	0.59**	0.58**	0.56**	0.53**	0.53**

[a] number concentration; [b] mass concentration;
*p<0.05; **p<0.01; ***p<0.001

Table 18. Total dust concentration (D_T) – Spearman's correlation coefficients between time-averaged measurements (impactors) and daily averages measured with DRIs

	D_T Sioutas						
	P-Trak®[a]	**DustTrak™ DRX[b]**					**DustTrak™ 8520[b]**
		PM_1	$PM_{2.5}$	PM_{Resp}	PM_{10}	PM_{Tot}	PM_{10}
M4 *n=12*	0.72*	0.77**	0.78**	0.77**	0.77**	0.73**	0.77**
M5 *n=12*	0.37	0.31	0.33	0.31	0.20	0.18	0.36
All *n=24*	0.47*	0.57**	0.60**	0.57**	0.55**	0.54**	0.61**

[a] number concentration; [b] mass concentration;
*p<0.05; **p<0.01; ***p<0.001

5.4.3 Paraffin wax fumes (M6)

Strong correlations were obtained between the paraffin wax measurements obtained from the Sioutas impactors and the daily averages of mass concentrations measured with DustTrak™ DRX and DustTrak™ 8520 (Table 19). The correlations with the daily averages of the number concentrations measured with the P-Trak® are slightly lower (r=0.6) but remain significant.

Table 19. Paraffin wax concentration -- Spearman's correlation coefficients between time-averaged measurements and daily averages measured with DRIs at M6

	Paraffin (C_{18}-C_{36}) Sioutas impactor						
	P-Trak®[a]	**DustTrak™ DRX[b]**					**DustTrak™ 8520[b]**
		PM_1	$PM_{2.5}$	PM_{Resp}	PM_{10}	PM_{Tot}	PM_{Tot}
M6 *n=12*	0.60*	0.93***	0.95***	0.94***	0.94***	0.94***	0.93***

[a] number concentration; [b] mass concentration;
*p<0.05; **p<0.01; ***p<0.001

5.4.4 Comparison of measurements – All workplaces (M1 to M6)

Figure 33 shows the relationships between the daily averages of the mass concentrations measured in the submicron fraction with DustTrak™ DRXs and the daily averages of the number concentrations measured with P-Traks®. Linear relationships can be seen, and they differ from one workplace to the next. M1 and M4 are characterized by high number concentrations, whereas their mass concentrations are generally below 1,000 µg/m³. Conversely, at M6, number concentrations remain relatively low (<100,000 particles/cm³) while mass concentrations are among the highest measured (between 500 and 1,500 µg/m³). These results suggest that particle size distributions are different in these workplaces.

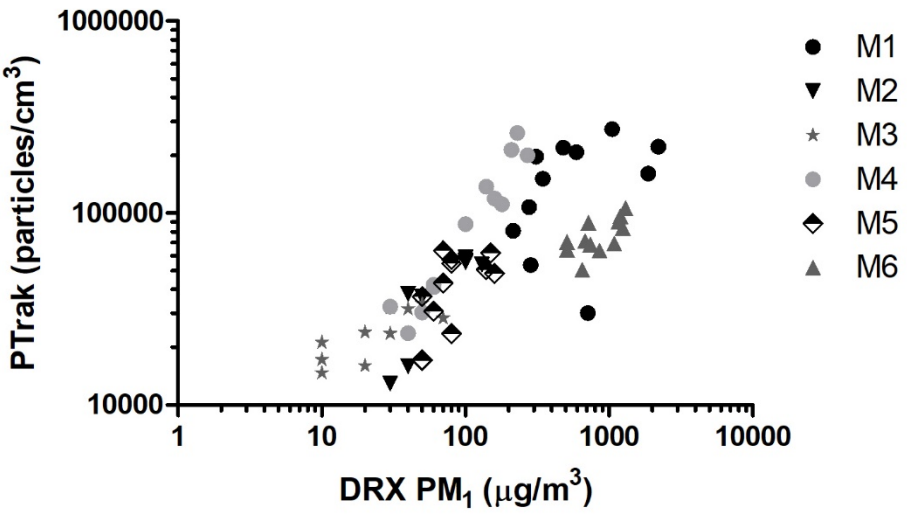

Figure 33. Relationship between mass concentrations measured with DustTrak™ DRXs and number concentrations measured with P-Traks®.

Figure 34 shows the distributions reported by the EEPS for M4 and M6 and the lower detection limit of the P-Trak® (as indicated in Table 2, the P-Trak® detects only particles larger than 20 nm). It can be seen from this figure that for M6, the vast majority of particles detected by the EEPS will also be detected with the P-Trak®. For M4, however, a significant proportion of particles were below the P-Trak® detection level, suggesting a potential underestimation of the number concentration there.

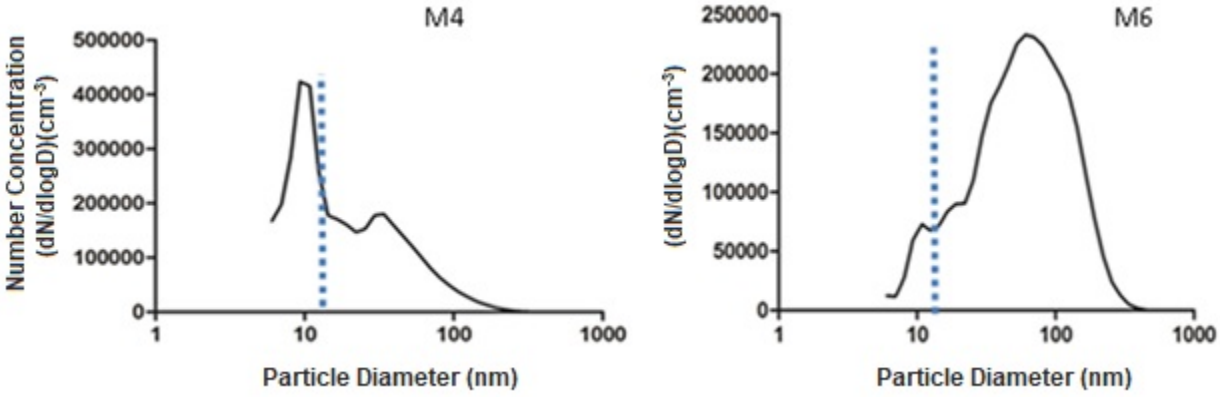

Dotted line represents lower limit of P-Trak®.

Figure 34. P-Trak® particle size distribution and detection limit.

5.5 Seasonal variations

In three of the six workplaces (M3, M4 and M6), large seasonal variations in the concentrations were observed. This type of variability was not seen in the other workplaces, i.e. the underground ones (M1 and M2) and those with no direct opening to the outside (M5).

For M3, when the measurements are separated by campaign, i.e. winter (D1, D2, D3) vs spring (D4, D5, D6), there are significant differences ($p<0.05$) between the time-averaged EC_R and EC_1 measurements, the winter values being at least three times higher than the spring ones (Figure 35). For M4, the fall measurements (D4, D5 and D6) were approximately 2.5 times higher than those measured during the summer season (D1, D2 and D3) ($p<0.05$), regardless of the sampling device used (37-mm cassette or Sioutas impactor) (Figure 36). For M6, the Sioutas measurements taken in the summer (D1, D2 and D3) were more than three times higher than those taken in the fall (D4, D5 and D6) ($p<0.05$).

At M3 and M4, the workplace layout allows significant changes in natural ventilation and air movement due to the opening (permanent in summer) of the many garage doors in the machine shop in the case of M3, and the opening of the accesses at either end of the foundry in the case of M4. In the case of M6, no difference in ventilation was observed, but higher concentrations were measured during the summer. These differences can be explained by the intensity of the work activities, which were different from one season to the next.

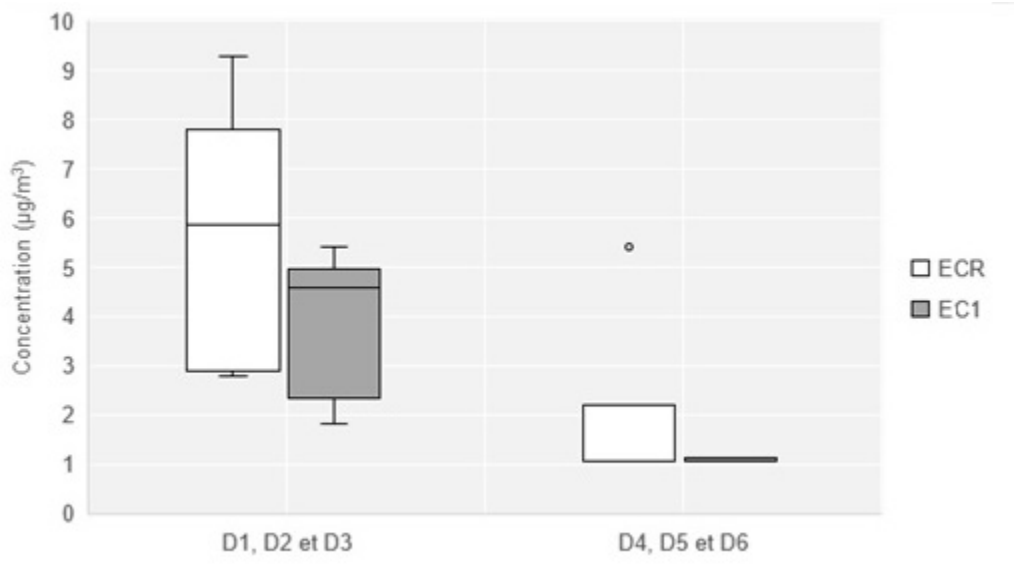

Figure 35. Distribution of winter measurements (closed doors, D1, D2 and D3) and spring measurements (open doors, D4, D5 and D6) of EC_R and EC_1 concentrations at M3.

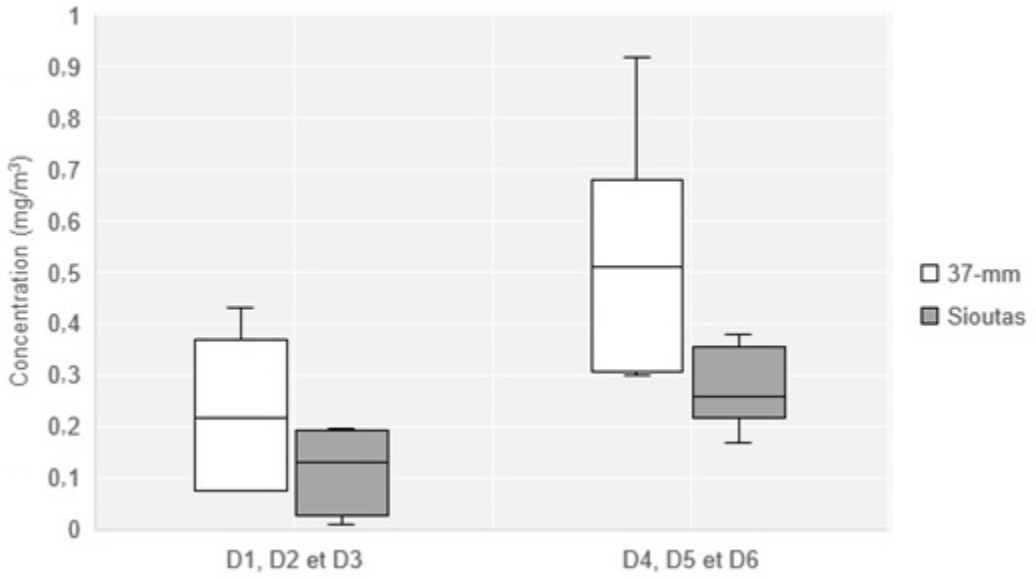

Figure 36. Distribution of summer measurements (open doors, D1, D2 and D3) and fall measurements (closed doors, D4, D5 and D6) of total dust collected with 37-mm cassettes or Sioutas impactors at M4.

6. DISCUSSION

This study provided an in-depth look at exposure to various types of URNPs in six workplaces in Québec. Through an innovative strategy using a wide range of methods and instruments, many indicators were measured in parallel. Number and mass concentration levels were measured using several DRIs. Time-averaged measurements were also taken, based on the type of contaminant specific to each workplace. These measurements included (i) respirable and submicron carbon (elemental and organic) fractions, as well as respirable combustible dust from DEE found in an underground mine (M1), in in maintenance operations in an underground transit system (M2) and in a truck repair garage(M3); (ii) gravimetric measurements and concentrations of 12 metals (aluminum, cadmium, chromium, cobalt, copper, iron, magnesium, manganese, nickel, lead, vanadium, zinc) in fumes and metallic dust released in a foundry (M4), as well as in a machine shop (welding, grinding and cutting) (M5); (iii) paraffin wax (C_{18}-C_{36}) from fumes released in a wax-moulding shop (M6). Measurements for the purpose of microscopic characterization were also taken in the six workplaces.

6.1 DEE at M1, M2 and M3

In the workplaces where DEE is present, the number concentrations observed were highly variable, with daily averages of 128,200 particles/cm³ [51,200-228,600], 32,800 particles/cm³ [12,900-58,600] and 22,800 particles/cm³ [14,700-33,800] for M1, M2 and M3 respectively. The levels observed at M2 and M3 were similar to those reported at port facilities (average daily concentration of 36,000 particles/cm^3, with a daily maximum of 67,000 particles/cm^3) and school bus garages (between 5,000 and 80,000 particles/cm^3) (Debia et al., 2016; Debia, Trachy-Bourget et al., 2017). At M1, on the other hand, the concentrations were higher and more comparable to those measured in environments with diesel-powered trains (average concentration of 126,000 particles/cm^3 and peak concentration of 693,000 particles/cm^3) or in underground parking garages (average concentration of 116,000 particles/cm^3 and peak concentration of 186,000 particles/cm^3) (Bujak-Pietrek, 2010; Jeong et al., 2017).

The mass concentration measurements obtained with DustTraks™ also cover a wide range of concentrations, with daily geometric means ranging from 0.01 to 3.48 mg/m³. At the above-mentioned port facilities, mean daily concentrations of 0.04 mg/m³ PM_{Resp} and 0.04 mg/m³ PM_1 have been recorded (Debia et al., 2016). In school bus garages, the mean daily concentrations ranged from 0.025 mg/m³ to 0.045 mg/m³ PM_{Resp} (Debia, Trachy-Bourget et al., 2017). These concentrations are of the same order of magnitude as those measured at M2 and M3; however, M1 again stands out with higher concentrations, having geometric means of 0.59 mg/m³ and 0.61 mg/m³ with the DustTrak™ 8520 and DustTrak™ DRX, respectively.

The TC levels measured in this study were lower than the Québec regulated level of 0.4 mg/m³ stipulated in the *Regulation Respecting Occupational Health and Safety in Mine*s, with the exception of a 0.7 mg/m³ level recorded at M1. In the mine (M1), concentrations were higher than some regulatory values, such as the one in force in Switzerland, with an EC_R limit of 0.1 mg/m³, regardless of the work environment. Fleck, Couture et al. (2018) recorded personal EC_R concentrations in two underground gold mines similar to the M1 environment in this study. They reported a personal workstation geometric mean EC_R of 0.083 mg/m^3, which is lower than the 0.137 mg/m^3 calculated for the same parameter in this study. Many of the workers in the Fleck et

al. study (2018) were in ventilated cabins with filtered air, which likely explains why the levels measured directly in their breathing zones were lower. In any case, the measurements taken in the present study cannot be used to draw conclusions about worker exposure, since they were strictly ambient measurements.

TC/EC ratios for diesel engine exhaust (DEE) are typically between 1.2 and 1.3 (Noll, Bugarski, Patts, Mischler and McWilliams, 2007), which is what we found at M1. However, higher ratios were reported for M2 and M3, indicating the potential for high occurrences of OCs not linked to diesel exhaust in these workplaces. The TC_R/EC_R ratios ranged from 2.36 to 5.33 while the TC_1/EC_1 ratios ranged from 2.4 to 5. At M2, the interference could come from oil residues deposited along the traffic lanes. At M3, it is highly likely that oil residues were also present since it is a truck garage. No cigarette smoke was detected during the visits to the first three workplaces. For M1, the average ratio of 1.37 suggests that OC is directly associated with DEE. Fleck et al. also reported ratios close to 1.3 in the underground mining environment. However, the ratios obtained for personal measurements in the same environment were higher and therefore likely to contain OC (Fleck, Couture et al., 2018). The authors attributed the interference to the presence of oil mist near equipment and workers.

The TC_1/TC_R and EC_1/EC_R ratios calculated for each of the three workplaces were greater than 0.5 (i.e., 50%) (see Table 10). In the mining environment, up to 97% of the carbon mass was in the submicron fraction. These ratios were in the range of 0.6 (60%) to 0.7 (70%) for the other two workplaces. These results indicate that the composition of DEF aerosols varies from one workplace to the next, but most the particulate mass is in the submicron fraction. Similar results were obtained by Fleck et al. (2018).

At M1, there was proportionally more non-combustible dust than in the other workplaces, with a CD_R/D_R ratio of 0.46. Ratios greater than 0.5 were calculated at M2 and M3. The mining environment is particularly likely to expose workers to rock dust, which would explain these results. In particular, silica dusts were observed there (see Figure 17). Rock dust would influence non-specific measurements obtained with DRIs such as the DustTrak™.

Overall, most of the DRIs showed good relationships with the EC_1 and EC_R measurements. These results indicate that DRIs can be good tools for quickly and cost-effectively assessing exposure levels or characterizing a workplace or workstation. However, they must be used with caution, and the person using them must understand their limitations and the corrections that may be required (see 5.4.1). Airtec appears to be a good instrument for rapidly assessing worker exposure to DEE, particularly in underground mining environments, by providing an EC_1 level directly comparable to regulatory or hygienic values. Other authors have noted the value of these instruments in assessing occupational exposure to DEE (Fleck, Couture et al., 2018; Noll and Janisko, 2013; Yu et al., 2015).

Microscopy images indicate the presence of chain-aggregated spherical carbon particles of different sizes. These observations are consistent with literature data that report the presence of chain-agglomerated spherical carbon particles with electric mobility diameters ranging from 50 to 300 nm. Those authors indicate that the equivalent aerodynamic diameters are 50 to 150 nm, with effective densities ranging from 1.6 to 0.25 g/cm³ (Leung et al., 2017; Park, Cao, Kittelson and McMurry, 2003). The particle size distribution of the number concentrations measured with the EEPS at M3 has two modes: one at 22.1 nm and one at 107.5 nm (see Figure 9). The second

mode seems to be more specifically associated with DEE since it predominates during peak particle concentrations (see Figure 10). This mode also corresponds to the particle sizes reported in the literature (Park et al., 2003).

Workers exposed to DEE are therefore exposed to mostly nanoscale airborne particles whose mass concentration is largely in the submicron fraction.

6.2 Metal fumes at M4 and M5

6.2.1 Foundry (M4)

In the production areas of the stainless steel foundry, daily mean concentrations ranging from 23,700 to 262,200 particles/cm^3 were measured with the P-Traks® while instantaneous concentrations ranging from 29,700 to 392,000 particles/cm^3 were measured with the EEPS. The main mode identified with the EEPS was 9.31 nm. Jarvela et al. also looked at particle emissions during the production of stainless steel and ferrochromium. They found comparable levels of particle concentrations in the production areas, ranging from 84,800 to 360,000 particles/cm^3 with a CPC3007 particle counter and from 101,000 to 2,740,000 particles/cm^3 with an SMPS (Jarvela et al., 2016). Debia et al. measured particle emissions during aluminum production, reporting average concentrations ranging from 70,000 to 144,000 particles/cm^3 depending on the production process (Debia, Weichenthal, Tardif and Dufresne, 2012). In short, there is considerable variability in concentration measurements. Many parameters may explain this variability, and several authors have attempted to explain their results using temporal profiles of concentrations and field observations. Jarvela et al. noted, for example, that measured concentrations were relatively stable, but dropped rapidly when the process was stopped (Jarvela et al. 2016). In the present study, large and statistically significant differences were observed in the foundry, depending on the season. Open doors allowed air to circulate freely in summer, whereas in winter the doors remained closed, resulting in a large increase in particle concentrations.

EEPS measurements indicate the presence of an abundance of ultrafine particles, with a main mode around 10 nm. These data are similar to those of Jarvela et al., who reported a main mode of less than 10 nm in the particle size distribution observed in foundries (Jarvela et al., 2016). Thomassen et al. reported a main mode of less than 20 nm in the particle size distributions occurring in pre-baked anode processes (Thomassen et al. 2006).

Time-averaged measurements yielded geometric mean concentrations of 0.188 mg/m^3 for the total fractions (37-mm cassette) and 0.135 mg/m^3 for fractions less than 10 µm (Sioutas). The maximum concentrations were 1.2 mg/m^3 and 0.56 mg/m^3, respectively. For information purposes, these maximum concentrations are below the regulatory or recommended thresholds for Particulates Not Otherwise Regulated (Table 20). They are also lower than the average 1.58 mg/m^3 reported in the literature for a stainless steel foundry (Jarvela et al., 2016).

A comparison of the metal concentrations with the recommendations of the American Conference of Governmental Industrial Hygienists (ACGIH, 2017) (Table 20) shows that all the concentrations are 10% below the recommended thresholds, even after corrective stoichiometric factors were applied (in the case of iron oxide, zinc oxide and vanadium pentoxide). The ACGIH also recommends a limit value for manganese in the respirable fraction. The average concentration

obtained for manganese with the Sioutas (fraction <10 µm, the closest to a respirable fraction) is about 50% of the ACGIH recommended limit. However, the data from this study are not directly comparable with the recommendations or with some of the levels reported in the literature, since they are ambient measurements. The exposure levels for manganese need to be checked in this workplace through personal measurements of the respiratory fraction in the workers' breathing zone.

Table 20. ACGIH recommended occupational exposure limit values (mg/m³) for metals (2017)

Particulates Not Otherwise Regulated (PNORs)	Chromium	Cobalt	Copper	Iron oxides	Manganese	Nickel	Lead metal	Vanadium pentoxide	Zinc oxide
10 (I) 3 (R)	0.5 (T)	0.02 (T)	0.2 (fumes) 1 (dust)	5 (R)	0.02 (R) 0.1 (I)	1.5 (I)	0.05 (T)	0.05 (I)	2 (R)

R: respirable fraction
I: inhalable fraction
T: total dust

Mass median aerodynamic diameters (MMAD) of less than 1 µm were calculated for the metals, and little difference was found from one sampling method to the next (IOM cassettes, 37-mm cassettes and Sioutas impactors). These results suggest that the aerosol in this workplace is very fine and most of the metal masses are in the submicron fraction.

The microscopy images show numerous spherical metallic particles of manganese, chromium, iron, nickel and silica. These spherical particles are either alone or in agglomerations of up to 10 or so particles ranging in size from a few dozen to a few hundred nanometres. They are similar to the particles found by other authors in the production of stainless steel and ferrochromium (Huvinen, 2001; Jarvela et al., 2016). Also noteworthy is the presence of needle-shaped zinc oxide particles similar to particles identified in a manganese alloy plant (Gjønnes et al., 2011).

In the presence of foundry fumes, workers are exposed to airborne particles that are mostly nanometric in size and whose mass concentration is chiefly in the <10 µm and submicronic fractions for chromium, cobalt, copper, iron, manganese, lead, vanadium and zinc.

6.2.2 Machine shop (M5)

Debia et al. (2014) previously described the number concentrations released during various welding operations and reported daily mean concentrations ranging from 50,000 to 150,000 particles/cm³, with peaks reaching the instrument ceiling of 500,000 particles/cm³. The measurements reported for M5 in the present study were lower on average, with mean concentrations of 41,000 particles/cm³ measured with the P-Trak® and 60,100 particles/cm³ with the EEPS. This is mainly due to the fact that we studied a machine shop where various activities take place, such as TIG welding, plasma cutting, grinding, joining and finishing. In welding schools such as those visited by Debia et al. (2014), large numbers of students perform a specific welding task simultaneously and for extended periods of time. Such a situation is not representative of the

working conditions of welders. The averages reported in the present study can be considered more representative of worker exposure in an industrial machine shop.

The time-averaged measurements yielded geometric mean concentrations of 0.321 mg/m^3 in the total fraction and 0.145 mg/m^3 in the <10 µm fraction (Sioutas). The maximum concentrations were 0.92 mg/m^3 and 0.38 mg/m^3, respectively. For information purposes only, these maximum concentrations are below the regulatory or recommended thresholds for PNORs (Table 20); they are also lower than the values reported in the literature, i.e. average concentrations of 7.14 mg/m³ for FCAW and 3.05 mg/m³ for GMAW welding processes (Hoffmeyer et al., 2012).

The measured metal concentrations were all less than 10% of the ACGIH recommended limit values (Table 20), even after corrective stoichiometric factors were applied (in the case of iron oxides, zinc oxides and vanadium pentoxide). Manganese levels were also nearly four times lower than those measured in the foundry (M4). Again, however, these data are not directly comparable with the guidelines or with some of the levels identified in the literature since they are ambient data whereas the guidelines apply to concentrations measured within the worker's breathing zone.

Mass measurements resulted in MMADs ranging from 0.2 to 2.4 µm for the different metals. The microscopy images show the presence of several types of particles, including many metallic oxide particles (manganese, chromium, iron, nickel and silica) of micrometric size and non-spherical shape (see Figure 27). The differences in concentrations between the IOM cassettes, 37-mm cassettes and Sioutas impactors suggest that micrometric particles are collected differently, depending on the sampling setup. Microscopy analyses show that the coarser particles are mostly found in the machining section close to the grinding operations. The results from sampling with the Sioutas (see Table 12) are similar to those of Kondej and Gaweda, who reported that most of the mass concentrations of aerosols generated during steel grinding were found at the coarsest stage of the impactor, i.e. from 2.5 to 10 µm (Kondej and Gaweda, 2012).

A second type of particle was identified at M5, this time near the welding and cutting operations. These were ultrafine particles agglomerated into chains hundreds of particles long (see Figure 26). The microscopy analyses show good correspondence with published work on particles generated during welding (Berlinger et al., 2011; Huvinen, 2001).

The levels measured with the EEPS indicate a main mode at 9.31 nm (see Figure 9). In a peak concentration situation, the second particle mode, which is at 34 nm, becomes more frequent. This second mode is likely associated with the generation of particulate matter in workplace M5, since it appears to be most influenced by changes in concentrations measured with the EEPS or other instruments. This second peak also corresponds to the particle sizes identified during electron microscopy observations.

The workers in M5 are therefore exposed to machining fumes and dust particles that are mainly nanometric in size, but some of the processes generate larger, micrometric particles. The contribution of larger particles to the mass concentration is significant in this environment and, as a result, the mass concentration is found in the inhalable fraction, especially for chromium, copper, iron and nickel.

6.3 Paraffin wax fumes at M6

M6 is characterized by particle concentrations close to 100,000 particles/cm^3. Of all the workplaces, it had the highest particle concentrations as measured with the DustTrak™ laser photometers (around 1 mg/m³). The main mode of the particle size distribution was 60.4 nm, and the average MMAD was 0.8 µm. Most of the particles ranged from a few hundred nanometres to a few micrometres, and they were rich in carbon.

Similar concentrations have been measured in a workplace where hot wax is applied to skis (Freberg et al., 2014). Using DRIs, the authors measured average concentrations of 1.07 mg/m³ in the respirable fraction and 1.62 mg/m³ in the inhalable fraction. However, they also measured average concentrations of 3.1 and 6.2 mg/m³ for the respirable and inhalable fractions, respectively, using filter (time-averaged) methods. When there was no ventilation, the number concentrations were 71,000 to 472,000 particles/cm³, with particle sizes ranging from 50 to 350 nm. The levels found in the present study are all below 0.37 mg/m³, which is much lower than those measured by Freberg et al. (2014). However, the analysis methods were not the same; Freberg et al. used a gravimetric method whereas we used a specific measurement method for paraffin wax (C_{18}-C_{36}) adapted from OSHA PV2047. The concentrations measured here were nonetheless well below the occupational exposure limit of 2 mg/m³ recommended by the ACGIH for paraffin wax fumes. No other studies conducted in an environment similar to M6 have been found in the literature. Further studies are therefore needed in environments where wax fumes are present.

Workers in the wax shop (M6) are thus exposed to carbon-rich fumes that are chiefly nanometric in size and whose mass concentration is mostly in the submicron fraction.

6.4 Considerations for ultrafine fraction measurement

Viitanen et al. (2017) recently identified the key factors for reliable measurement of URNPs in the workplace. The authors first recognized a lack of URNP measurements in workplaces, primarily due to the absence of a specific exposure limit value and the lack of sampling methods and tools. They also pointed out the lack of a standard method for measuring particles less than 20 nm in diameter.

In addition, they identified several issues inherent in the assessment of occupational exposure to URNPs. These include the significant impact of ventilation parameters, the treatment of background noise and the presence of other particles that are not of interest or are not nanoscale. Finally, the authors identified a need to conduct parallel measurements using different techniques in order to improve the understanding of URNP assessments. The present study provides information and reflections related to these issues.

We conducted repeated assessments in six different settings. Repetition enabled the variability of exposure levels to be characterized and average levels to be specified. Through repetition we were also able to characterize seasonal variations in contamination levels in two of the six workplaces (M3 and M4). Using the indicators assessed, we were able to identify the seasonal variations and link them to the presence of natural ventilation during warmer times of the year. Variability across sampling periods was also found at M6, but it was not associated with any changes in environmental conditions.

The number concentrations were determined by means of a CNC (P-Trak®) and an EEPS. Differences are noted between the concentrations reported, and they appear to increase at higher concentrations. Zhu et al. have shown that the P-Trak® is generally effective in measuring URNP exposure compared to other more sensitive but not portable instruments, except at very high concentrations (Zhu, Yu, Kuhn and Hinds, 2006). Many authors also use counters that measure particle aerodynamic diameters. These instruments require the use of effective density to indicate number and mass concentrations and to compare aerodynamic and electric mobility diameters (Park et al., 2003). However, it remains difficult to determine a single effective density for an industrial aerosol that can be polydispersed and may be varied in chemical composition. In this study, an ELPI was also tested at M4 (data not presented). The concentrations reported with a density of 1 (GM of 15,000 particles/cm³) were much lower than the concentrations obtained with the EEPS (GM of 222,000 particles/cm³) and the P-Trak® (GM of 83,362 particles/cm³). However, when a density of 5 was considered, the concentrations became comparable and increased from 15,000 particles/cm³ to 160,000 particles/cm³. Some authors propose methodologies to determine this effective density and establish the correspondence between the different types of diameters (aerodynamic/electrical/physical), but further studies are needed to better interpret these results and remove the uncertainties. Comparing the number concentrations obtained with different instruments therefore remains a major issue for the assessment of occupational exposure.

This study also showed the advantage of developing DRIs specifically for measuring a contaminant. Measurements obtained with the FLIR Airtec are of great interest for the assessment of DEF exposure since they are accurate and provide the user with a direct comparison with limit values expressed in EC_1.

Parallel measurements of concentrations according to different fractions (PM_1, PM_{Resp}, PM_{10}, PM_{Tot}) also resulted in better understanding of the variations in mass concentrations between these indicators. While differences were noted between the fractions for DEE (M2 and M3 only) and machining fumes and dusts (M5), little variation was observed for foundry fumes and mine DEE (M1) (see Table 9 and Table 13). These results obviously reflect the impact of aerosol particle size distribution on mass measurement, but also suggest the need to develop harmonized methods to evaluate an ultrafine fraction that would have an impact on the respiratory health of workers. As presented in 2.3.2.1, the nanoparticle respiratory deposition sampler (NRD) is intended to address this issue by sampling a specific fraction of an aerosol--essentially, the ultrafine fraction that would be deposited in the respiratory tract. Little published data is available on this sampler, which, to the best of our knowledge, has been used only in studies of metal fumes (Cena et al., 2015; Cena, Chisholm, Keane, Cumpston and Chen, 2014).

Microscopy studies have yielded accurate characterizations of the collected particles. Several hundred analyses of the morphology and nature of the observed particles were carried out during this study. In 2016, Debia et al. recommended analyzing about 20 particles per microscopy grid to confirm the presence of MNPs and perform an elemental characterization of the collected particles (Debia, L'Espérance, et al., 2017). The recommendation was applied in this study, as 21 particles were analyzed per grid. Very good homogeneity was observed between the workplaces evaluated for each grid. These results suggest that the recommendation of analyzing about 20 particles per grid would be sufficient to characterize the nature of the URNPs in a workplace.

Particle samples on microscopy grids were taken using Mini Particle Samplers. R'Mili et al. evaluated the collection capacity of a Mini Particle Sampler at flow rates of 0.3 L/min and with Quantifoil microscopy grids, a protocol similar to the one used in this study (R'mili, Dutouquet, Sirven, Aguerre-Chariol and Frejafon, 2011). They reported sample collections with relatively low efficiencies for particles between 5 and 150 nm. The particles collected on the grids may not have been representative of the overall airborne particles present in the workplace. Nevertheless, a Mini Particle Sampler is still appropriate for industrial hygiene assessments because of its simplicity of use and its effectiveness in reproducing results, as highlighted in this study. Further studies are still needed to standardize particle analysis by electron microscopy.

7. CONCLUSION

The objective was to evaluate various situations of potential exposure to URNPs in six Québec workplaces.

The DRI measurements yielded daily number concentrations ranging between 12,900 and 228,600 particles/cm³ and mass concentrations between 0.01 and 3.22 mg/m³ for the six workplaces. The underground mine was the environment with the highest concentrations in terms of number of particles, while the wax-moulding shop had the highest mass concentrations. In environments where DEE was found, daily concentrations of EC_1 ranging from 0.002 to 0.503 mg/m³ were measured with DRIs.

Time-averaged measurements were also carried out in order to determine the environmental concentrations. For information purposes only, the TC concentrations measured in this study were lower than the 0.4 mg/m³ stipulated in the Québec *Regulation Respecting Occupational Health and Safety in Mines*, with the exception of a level of 0.7 mg/m³ recorded in workplace M1. It was found that all the metal concentrations in workplaces M4 and M5 were less than 10% of the threshold values recommended by the ACGIH. The only exception was the manganese level measured with the Sioutas impactor in the foundry (M4); it was above the ACGIH recommendation for the respirable fraction of manganese. The paraffin wax fumes measured were below the occupational exposure limit of 2 mg/m³ set by the ACGIH.

Workers exposed to DEE (M1, M2 and M3) are exposed to mostly nanometric-size airborne particles whose mass concentration is largely in the submicron fraction. In the presence of foundry fumes (M4), workers are exposed to airborne particles that are mostly nanometric in size and whose mass concentration is chiefly in the submicron fraction for chromium, cobalt, copper, iron, manganese, lead, vanadium and zinc. The workers at M5 are exposed to machining fumes and dust particles that are mainly nanometric in size, but some of the processes generate larger, micrometric particles. The contribution of larger particles to the mass concentration is significant in this environment and, as a result, the mass concentration is found mainly in the inhalable fraction, especially for chromium, copper, iron and nickel. Workers in the wax shop (M6) are exposed to fumes that are chiefly nanometric in size and whose mass concentration is mostly in the submicron fraction.

Microscopy studies yielded accurate characterizations of the collected particles. The particulate matter identified at M1, M2 and M3 indicated the presence of chain-agglomerated spherical carbon particles of different sizes. The particles identified at the foundry (M4) were essentially spherical ranging from 50 to 500 nm, isolated or in agglomerates of up to about 10 particles, and composed mostly and quite consistently of metal oxides predominated by iron, chromium, manganese, zinc, copper, aluminum, nickel and lead. The particles identified in the machining shop (M5) were of various shapes and compositions. There were two main types of particles: the first were very fine particles, on the order of a few nanometres, highly agglomerated in chains. They were mainly found on sample grids taken near welding and arc cutting operations. These particles contained mainly iron, copper, silicon, chromium, manganese, nickel and, more rarely, potassium, sulphur, phosphorus and chlorine. The second category consisted of particles of various shapes, non-specific or non-spherical, rather coarse (0.5 to 5 µm) and with various chemical compositions. They were mainly found on sample grids taken near grinding operations.

These particles contained mainly iron, aluminum, silicon, chromium, nickel, manganese, titanium and, more rarely niobium, potassium and zirconium. The particles identified in the wax shop (M6) were carbon-rich and of various shapes ranging from near spherical to rod-shaped. They ranged in size from a few hundred nanometres to a few micrometres.

Our innovative strategy enabled us to accurately characterize the URNPs released in the workplaces in terms of number and mass concentrations, morphology and chemical composition. Differences are noted between the number concentrations reported by a CNC (P-Trak®) and an EEPS. Comparing the number concentrations obtained with different instruments therefore remains a major issue for the assessment of occupational exposure. Following particle sampling with an MPS on microscopy grids, microscopy analyses led to accurate characterizations. A Mini Particle Sampler remains adequate for occupational hygiene assessments because of its simplicity of use and its effectiveness in reproducing results, as highlighted in this study.

BIBLIOGRAPHY

Andersen, Z. J., Loft, S., Ketzel, M., Stage, M., Scheike, T., Hermansen, M. N. and Bisgaard, H. (2008). Ambient air pollution triggers wheezing symptoms in infants. *Thorax, 63*(8), 710-716. doi: 10.1136/thx.2007.085480

Atkinson, R. W., Fuller, G. W., Anderson, H. R., Harrison, R. M. and Armstrong, B. (2010). Urban ambient particle metrics and health: A time-series analysis. *Epidemiology*, *21*(4), 501-511. doi: 10.1097/EDE.0b013e3181debc88

Bakand, S., Hayes, A. and Dechsakulthorn, F. (2012). Nanoparticles: A review of particle toxicology following inhalation exposure. *Inhalation Toxicology, 24*(2), 125-135. doi: 10.3109/08958378.2010.642021

Barclay, J. L., Miller, B. G., Dick, S., Dennekamp, M., Ford, I., Hillis, G. S., ... Seaton, A. (2009). A panel study of air pollution in subjects with heart failure: Negative results in treated patients. *Occupational and Environmental Medicine*, *66*(5), 325-334. doi: 10.1136/oem.2008.039032

Bello, D., Wardle, B. L., Yamamoto, N., Devilloria, R. G., Garcia, E. J., Hart, A. J.,... Hallock, M. (2009). Exposure to nanoscale particles and fibers during machining of hybrid advanced composites containing carbon nanotubes. *Journal of Nanoparticle Research*, *11*(1), 231-249.

Bello, D., Wardle, B.L., Zhang, J., Yamamoto, N., Santeufemio, C., Hallock, M. and Virji, M.A. (2010). Characterization of exposures to nanoscale particles and fibers during solid core drilling of hybrid carbon nanotube advanced composites. *International Journal of Occupational & Environmental Health, 16*(4), 434-450.

Benbrahim-Tallaa, L., Baan, R. A., Grosse, Y, Lauby-Secretan, B., El Ghissassi, F. and Bouvard, V. (2012). Carcinogenicity of diesel-engine and gasoline-engine exhausts and some nitroarenes. *Lancet Oncology, 13*(7), 663-664.

Berlinger, B., Benker, N., Weinbruch, S., L'Vov, B., Ebert, M., Koch, W., ... Thomassen, Y. (2011). Physicochemical characterisation of different welding aerosols. *Analytical and Bioanalytical Chemistry, 399*(5), 1773-1780.

Breitner, S., Liu, L., Cyrys, J., Brüske, I., Franck, U., Schlink, U., ... Hu, M. (2011). Sub-micrometer particulate air pollution and cardiovascular mortality in Beijing, China. *Science of the Total Environment*, *409*(24), 5196-5204. doi: 10.1016/j.scitotenv.2011.08.023

Breitner, S., Stolzel, M., Cyrys, J., Pitz, M., Wölke, G., Kreyling, W., ... Peters, A. (2009). Short-term mortality rates during a decade of improved air quality in Erfurt, Germany. *Environmental Health Perspectives, 117*(3), 448-454. doi: 10.1289/ehp.11711

Brouwer, D., Berges, M., Virji, M. A., Fransman, W., Bello, D., Hodson, L., ... Tielemans, E. (2012). Harmonization of measurement strategies for exposure to manufactured nano-objects: Report of a workshop. *Annals of Occupational Hygiene, 56*(1), 1-9. doi: 10.1093/annhyg/mer099

Brouwer, D. H., Gijsbers, J. H. and Lurvink, M. W. (2004). Personal exposure to ultrafine particles in the workplace: Exploring sampling techniques and strategies. *Annals of Occupational Hygiene, 48*(5), 439-453.

Bujak-Pietrek, S. (2010). Occupational exposure to nanoparticles: Assessment of workplace exposure. *Medycyna Pracy*, *61*(2), 183-189.

Bujak-Pietrek, S., Mikolajczyk, U., Kaminska, I. *,* Cieslak, M. and Szadkowska-Stanczyk, I. (2016). Exposure to diesel exhaust fumes in the context of exposure to ultrafine particles. *International Journal of Occupational Medicine and Environmental Health, 29*(4), 667-682.

Cattaneo, A., Garramone, G., Taronna, M., Perruzo, C. and Cavallo, D. M. (2009). Personal exposure to airborne ultrafine particles in the urban area of Milan. *Journal of Physics, 151*(1), 012039. From https://iopscience.iop.org/article/10.1088/1742-6596/151/1/012039

Cena, L. G., Chisholm, W. P., Keane, M. J. and Chen, B. T. (2015). A field study on the respiratory deposition of the nano-sized fraction of mild and stainless steel welding fume metals. *Journal of Occupational and Environmental Hygiene, 12*(10), 721-728. doi: 10.1080/15459624.2015.1043055

Cena, L. G., Chisholm, W. P., Keane, M. J., Cumpston, A. and Chen, B. T. (2014). Size distribution and estimated respiratory deposition of total chromium, hexavalent chromium, manganese and nickel in gas metal arc welding fume aerosols. *Aerosol Science and Technology*, *48*(12), 1254-1263.

Cena, L. G. and Peters, T. M. (2011). Characterization and control of airborne particles emitted during production of epoxy/carbon nanotube nanocomposites. *Journal of Occupational and Environmental Hygiene, 8*(2), 86-92.

Dahm, M.M., Yencken, M.S. and Schubauer-Berigan, M.K. (2011). Exposure control strategies in the carbonaceous nanomaterial industry. *Occupational and Environmental Medicine, 53*(6 S), S68-S73.

De Hartog, J. J., Ayres, J. G., Karakatsani, A., Analitis, A., Ten Brink, H., Hameri, K., ... Meddings, C. (2010). Lung function and indicators of exposure to indoor and outdoor particulate matter among asthma and COPD patients. *Occupational and Environmental Medicine, 67*(1), 2-10. doi: 10.1136/oem.2008.040857

Debia, M., Beaudry, C., Weichenthal, S., Tardif, R. and Dufresne, A. (2012a). *Characterization and Control of Occupational Exposure to Nanoparticles and Ultrafine Parti*cles (Report No. R-746). Montreal, QC: IRSST

Debia, M., Beaudry, C., Weichenthal, S., Tardif, R. and Dufresne, A. (2012b). Exposure to ultrafine particles in the pre-baked anode process of an aluminium smelter. *Labour & Health, 28*(4), S12-S17.

Debia, M., L'Espérance, G., Catto, C., Plamondon, P., Dufresne, A and Ostiguy, C. (2017). *Évaluation de méthodes de prélèvement et de caractérisation de nanomatériaux manufacturés dans l'air et sur des surfaces des milieux de travail* (Report No. R-952). Montreal, QC*:* IRSST

Debia, M., Neesham-Grenon, E., Mudaheranwa, O.C. and Ragettli, M.S. (2016). Diesel exhaust exposures in port workers. *Journal of Occupational and Environmenatal Hygiene, 13*(7), 549-557. doi: 10.1080/15459624.2016.1153802

Debia, M., Trachy-Bourget, M. C., Beaudry, C., Neesham-Grenon, E., Perron, S. and Lapointe, C. (2017). Characterization of indoor diesel exhaust emissions from the parking garage of a school. *Environmental Science and Pollution Research, 24*(5), 4655-4665. doi: 10.1007/s11356-016-8129-4

Debia, M., Weichenthal, S. and Dufresne, A. (2014). Case study: Ultrafine particles exposure in apprentice welders. *Journal of Occupational and Environmental Hygiene, 11*(1), D1-9. doi: 10.1080/15459624.2013.836280

Debia, M., Weichenthal, S., Tardif, R. and Dusfresne, A. (2012). Ultrafine Particle (UFP) Exposures in an aluminium smelter: Soderberg vs. prebake potrooms. *Environment and Pollution, 1*(1), 2-12.

Delfino, R.J., Gillen, D.L., Tjoa, T., Staimer, N., Polidori, A., Arhami, M., ... Longhurst, J. (2011). Electrocardiographic ST-segment depression and exposure to traffic-related aerosols in elderly subjects with coronary artery disease. *Environmental Health Perspectives, 119*(2), 196-202. doi: 10.1289/ehp.1002372

Delfino, R.J., Staimer, N., Tjoa, T., Gillen, D.L., Polidori, A., Arhami, M., ... Sioutas, C. (2009). Air pollution exposures and circulating biomarkers of effect in a susceptible population: Clues to potential causal component mixtures and mechanisms. *Environmental Health Perspectives, 117*(8), 1232-1238. doi: 10.1289/ehp.0800194

Dewalle, P., Vendel, J., Weulersse, J.-M., Hervé, P. and Decobert, G. (2010). Characterization of aerosols generated by nanosecond laser ablation of an acrylic paint. *Aerosol Science and Technology, 44*(10), 902-915.

Dierschke, K., Isaxon, C., Andersson, U. B.K., Assarsson, E., Axmon, A., Stockfelt, L., ... Pagels, J. (2017). Acute respiratory effects and biomarkers of inflammation due to welding-derived nanoparticle aggregates. *International Archives of Occupational and Environmental Health, 90*(5), 451-463. doi: 10.1007/s00420-017-1209-z

Evans, D.E., Ku, B.K., Birch, M.E. and Dunn, K.H. (2010). Aerosol monitoring during carbon nanofiber production: Mobile direct-reading sampling. *Annals of Occupational Hygiene*, *54*(5), 514-531.

Fleck, A., Cabelguen, V., Couture, C., Lachapelle, G., Ryan, P., Thuot, R. and Debia, M. (2019). Comparison between personal sampling methodologies for evaluating diesel particulate matter exposures in mines: Submicron total carbon corrected for the adsorption of vapor-phase organic carbon vs. respirable total carbon. *Journal of Occupational and Environmental Hygiene*, *16*(1), 1-14. doi: 10.1080/15459624.2018.1532576

Fleck, A., Couture, C., Sauvé, J.F., Njanga, P.E., Neesham-Grenon, E., Lachapelle, G., ... Debia, M. (2018). Diesel engine exhaust exposure in underground mines: Comparison between different surrogates of particulate exposure. *Journal of Occupational and Environmental Hygiene*, *15*(7), 549-558.

Frampton, M.W., Utell, M.J., Zareba, W., Oberdörster, G., Cox, C., Huang, L.S., ... Stewart, J. (2004). Effects of exposure to ultrafine carbon particles in healthy subjects and subjects with asthma (Report No. 126). Boston, MA: Health Effects Institute.

Freberg, B.I., Olsen, R., Daae, H.L., Hersson, M., Thorud, S., Ellingsen, D.G. and Molander, P. (2014). Occupational exposure assessment of airborne chemical contaminants among professional ski waxers. *Annals of Occupational Hygiene*, *58*(5), 601-611. doi: 10.1093/annhyg/meu015

Freund, A., Zuckerman, N., Baum, L. and Milek, D. (2012). Submicron particle monitoring of paving and related road construction operations. *Journal of Occupational and Environmental Hygiene*, *9*(5), 298-307. doi: 10.1080/15459624.2012.672924

Gjønnes, K., Skogstad, A., Hetland, S., Ellingsen, D. G., Thomassen, Y. and Weinbruch, S. (2011). Characterization of workplace aerosols in the manganese alloy production industry by electron microscopy. *Analytical and Bioanalytical Chemistry*, *399*(3), 1011-1020.

Gong, J., Zhu, T., Kipen, H., Wang, G., Hu, M., Guo, Q., ... Rich, D.Q. (2014). Comparisons of ultrafine and fine particles in their associations with biomarkers reflecting physiological pathways. *Environmental Science & Technology*, *48*(9), 5264-5273. doi: 10.1021/es5006016

Guha, N., Loomis, D., Guyton, K. Z., Grosse, Y., El Ghissassi, F., Bouvard, V., ... Straif, K. (2017). Carcinogenicity of welding, molybdenum trioxide, and indium tin oxide. *The Lancet Oncology*, *18*(5), 581-582. doi: 10.1016/s1470-2045(17)30255-3

Haluza, D., Moshammer, H. and Hochgatterer, K. (2014). Dust is in the air: Part II: Effects of occupational exposure to welding fumes on lung function in a 9-year study. *Lung, 192*(1), 111-117. doi: 10.1007/s00408-013-9529-6

Handy, R.G., Jackson, M.J., Robinson, G.M. and Lafreniere, M.D. (2006). The measurement of ultrafine particles: A pilot study using a portable particle counting technique to measure generated particles during a micromachining process. *Journal of Materials Engineering and Performance, 15*(2), 172-177.

Hinds, W.C. (1998). *Aerosol technology: Properties, behavior, and measurement of airborne particles* (2nd ed.). New York, NY: John Wiley & Sons.

Hoffmeyer, F., Raulf-Heimsoth, M., Lehnert, M., Kendzia, B., Bernard, S., Berresheim, H., ... Pesch, B. (2012). Impact of different welding techniques on biological effect markers in exhaled breath condensate of 58 mild steel welders. *Journal of Toxicology and Environmental Health, A*, *75*(8-10), 525-532. doi: 10.1080/15287394.2012.675303

Huvinen, M. (2001). Surface structure and speciation of metal aerosols: A key to the understanding of their biological effects. In L. Ebdon, L. Pitts, R. Cornelis, H. Crews, O. F. X. Donard, P. Quevauviller (Eds.), *Trace element speciation for environment, food and health* (pp. 308-314). Cambridge, England: RSC.

International Agency for Research on Cancer. (2014). *Diesel and gasoline engine exhausts and some nitroarenes*. From https://monographs.iarc.fr/wp-content/uploads/2018/06/mono105.pdf

Järvelä, M., Huvinen, M., Viitanen, A.K., Kanerva, T., Vanhala, E., Uitti, J., ... Tuomi, T. (2016). Characterization of particle exposure in ferrochromium and stainless steel production. *Journal of Occupational and Environmental Hygiene*, *13*(7), 558-568.

. Järvelä, M., Huvinen, M., Viitanen, A.K., Kanerva, T., Vanhala, E., Uitti, J., ... Tuomi, T. (2016). Characterization of particle exposure in ferrochromium and stainless steel production. *Journal of Occupational and Environmental Hygiene*, *13*(7), 558-568. doi: 10.1080/15459624.2016.1159687

Jeong, C.-H., Traub, A. and Evans, G. J. (2017). Exposure to ultrafine particles and black carbon in diesel-powered commuter trains. *Atmospheric Environment, 155*, 46-52.

Jorgensen, R.B., Buhagen, M. and Foreland, S. (2016). Personal exposure to ultrafine particles from PVC welding and concrete work during tunnel rehabilitation. *Occupational and Environmental Medicine, 73*(7), 467-473. doi: 10.1136/oemed-2015-103411

Karottki, D.G., Bekö, G., Clausen, G., Madsen, A.M., Andersen, Z.J., Massling, A., ... Møller, P. (2014). Cardiovascular and lung function in relation to outdoor and indoor exposure to fine and ultrafine particulate matter in middle-aged subjects. *Environment International*, *73*, 372-381. doi: 10.1016/d.env.2014.08.019

Kim, J.Y., Magari, S.R., Herrick, R.F., Smith, T.J., Christiani, D.C. and Christiani, D.C. (2004). Comparison of fine particle measurements from a direct-reading instrument and a gravimetric sampling method. *Journal of Occupational and Environmental Hygiene*, *1*(11), 707-715. doi: 10.1080/15459620490515833

Koivisto, A.J. (2010). Impact of particle emissions of new laser printers on modeled office room. *Atmospheric Environment, 44*(17), 2140-2146.

Kondej, D. and Gaweda, E. (2012). Metals in dust fractions emitted at mechanical workstations. *International Journal of Occupational Safety and Ergonomics, 18*(4), 453-460. doi: 10.1080/10803548.2012.11076952

Kouassi, S., Catto, C., Ostiguy, C., L'Espérance, G., Kroeger, J. and Debia, M. (2017). Exposure assessment in a single-walled carbon nanotube primary manufacturer. *Annals of Work Exposures and Health*, *61*(2), 260-266.

Kreyling, W.G., Semmler-Behnke, M., Takenaka, S. and Möller, W. (2012). Differences in the biokinetics of inhaled nano- versus micrometer-sized particles. *Accounts of Chemical Research*, *46*(3), 714-722. doi: 10.1021/ar300043r

Kuhlbusch, T.A. and Fissan, H. (2006). Particle characteristics in the reactor and pelletizing areas of carbon black production. *Journal of Occupational Environmental Hygiene, 3*(10), 558-567. doi: 10.1080/15459620600912280

Kuhlbusch, T. A., Neumann, S. and Fissan, H. (2004). Number size distribution, mass concentration, and particle composition of PM_1, $PM_{2.5}$, and PM_{10} in bag filling areas of carbon black production. *Journal of Occupational and Environmental Hygiene, 1*(10), 660-671.

Leung, K.K., Schnitzler, E.G., Dastanpour, R., Rogak, S.N., Jäger, W. and Olfert, J.S. (2017). Relationship between coating-induced soot aggregate restructuring and primary particle number. *Environmental Science & Technology*, *51*(15), 8376-8383. doi: 10.1021/acs.est.7b01140

NIOSH. (2003). Diesel particulate matter (as Elemental Carbon). In *NIOSH Manual of Analytical Methods* (4th ed.). From https://www.cdc.gov/niosh/docs/2003-154/pdfs/5040.pdf

Noll, J.D., Bugarski, A.D., Patts, L.D., Mischler, S.E. and McWilliams, L. (2007). Relationship between elemental carbon, total carbon, and diesel particulate matter in several underground metal/non-metal mines. *Environmental Science & Technology*, *41*(3), 710-716.

Noll, J. and Janisko, S. (2013). Evaluation of a wearable monitor for measuring real-time diesel particulate matter concentrations in several underground mines. *Journal of Occupational and Environmental Hygiene, 10*(12), 716-722.

Ostiguy, C., Debia, M., Roberge, B. and Dufresne, A. (2014). *Nanomaterials*: *Good Practice Guide for Risk Management in the Workplace* (2nd ed., Report No. R-840). Montréal, QC: IRSST

Park, K., Cao, F., Kittelson, D.B. and McMurray, P.H. (2003). Relationship between particle mass and mobility for diesel exhaust particles. *Environmental Science & Technology, 37*(3), 577-583.

R'mili, B., Dutouquet, C., Sirven, J.B., Aguerre-Chariol, O. and Frejafon, E. (2011). Analysis of particle release using LIBS (laser-induced breakdown spectroscopy) and TEM (transmission electron microscopy) samplers when handling CNT (carbon nanotube) powders. *Journal of Nanoparticle Research*, *13*(2), 563-577.

Raynor, P.C., Cebula, J.I., Spangenberger, J.S., Olson, B.A., Dasch, J.M. and D'Arcy, J.B. (2012). Assessing potential nanoparticle release during nanocomposite shredding using direct-reading instruments. *Journal of Occupational and Environmental Hygiene*, *9*(1), 1-13. doi: 10.1080/15459624.2012.633061

Rich, D.Q., Zareba, W., Beckett, W., Hopke, P.K., Oakes, D., Frampton, M.W., ... Wang, Y. (2012). Are ambient ultrafine, accumulation mode, and fine particles associated with adverse cardiac responses in patients undergoing cardiac rehabilitation?. *Environmental Health Perspectives*, *120*(8), 1162-1169. doi: 10.1289/ehp.1104262

Schmoll, L.H., Peters, T.M. and O'Shaughnessy, P.T. (2010). Use of a condensation particle counter and an optical particle counter to assess the number concentration of engineered nanoparticles. *Journal of Occupational and Environmental Hygiene, 7*(9), 535-545. From https://www.tandfonline.com/doi/full/10.1080/15459624.2010.496072

Song, S., Lee, K., Lee, Y.M., Lee, J.H., Lee, S.I., Yu, S.D. and Paek, D. (2011). Acute health effects of urban fine and ultrafine particles on children with atopic dermatitis. *Environmental Research*, *111*(3), 394-399. doi: 10.1016/d.envres.2010.10.010

Szymczak, W., Menzel, N. and Keck, L. (2007). Emission of ultrafine copper particles by universal motors controlled by phase angle modulation. *Journal of Aerosol Science, 38*(5), 520-531.

Thomassen, Y., Koch, W., Dunkhorst, W., Ellingsen, D.G., Skaugset, N.P., Jordbekken, L., ... Weinbruch, S. (2006). Ultrafine particles at workplaces of a primary aluminium smelter. *Journal of Environmental Monitoring*, *8*(1), 127-133.

Viitanen, A.K., Uuksulainen, S., Koivisto, A.J., Hämeri, K. and Kauppinen, T. (2017). Workplace measurements of ultrafine particles: A literature review. *Annals of Work Exposures and Health*, *61*(7), 749-758. doi: 10.1093/annweh/wxx049

Yu, C. H., Patton, A. P., Zhang, A., Fan, Z. H., Weisel, C. P. and Lioy, P. J. (2015). Evaluation of diesel exhaust continuous monitors in controlled environmental conditions. *Journal of Occupational and Environmental Hygiene*, *12*(9), 577-587.

Zhu, Y., Yu, N., Kuhn, T. and Hinds, W. C. (2006). Field comparison of P-Trak and condensation particle counters. *Aerosol Science and Technology*, *40*(6), 422-430.